Electronic supporting information

for

Fully reversible three-state interconversion of metallosupramolecular architectures

Nikita Mittal, Manik Lal Saha and Michael Schmittel*

Center of Micro and Nanochemistry and Engineering, Organische Chemie I,

Universität Siegen, Adolf-Reichwein-Str. 2, D-57068 Siegen, Germany.

E-mail: schmittel@chemie.uni-siegen.de

Table of Contents

DCM: dichloromethane

Synthesis

General

All commercial reagents were used without further purification. Solvents were dried with the appropriate desiccants and distilled prior to use. Silica gel (60-230 mesh) was used for column chromatography. ^{1}H NMR and ^{13}C NMR were recorded on a Bruker Avance 400 MHz using the deuterated solvent as the lock and residual protiated solvent as the internal reference (CD_2Cl_2: δ_H = 5.32 ppm and δ_C = 53.8 ppm). DOSY NMR spectra were recorded on a Varian VNMR-S 600 MHz. The following abbreviations were utilised to describe peak patterns: s = singlet, d = doublet, t = triplet, dd = doublet of doublet, td = triplet of doublet, dt = doublet of triplet, br = broad, bs = broad singlet, bd = broad doublet and m = multiplet. The numbering of the carbon atoms in the molecular formulae (*vide infra*) is only used for the assignments of the NMR signals and is not in accordance with IUPAC nomenclature rules. Electrospray ionisation mass spectra (ESI-MS) were recorded on a Thermo-Quest LCQ Deca. Melting points were measured on a Büchi SMP-20 instrument. Infrared spectra were recorded using a Varian 1000 FT-IR instrument. Elemental analysis was done on the EA 3000 CHNS. Energy minimised structures were obtained using the MM^{+} forced field as implemented in Hyperchem® 8.0. Ligands **2**,[1] **3**,[2] **5**,[3] and **9**[2] were synthesised according to known procedures.

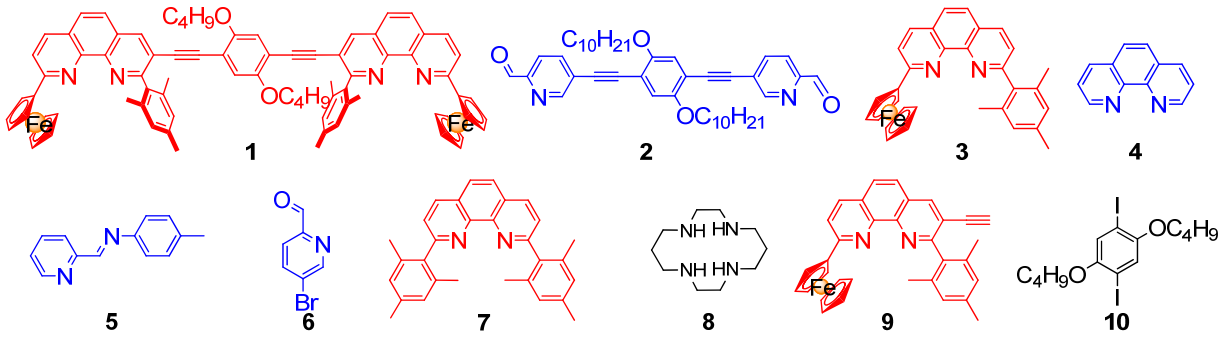

Chart 1: Chemical structures of the compounds **1**-**10** used in the current study.

9-(Ferrocenyl)-3-((2,5-dibutoxy-4-((9-(ferrocenyl)-2-mesityl-1,10-phenanthrolin-3-yl)ethynyl)phenyl)ethynyl)-2-mesityl-1,10-phenanthroline (1)

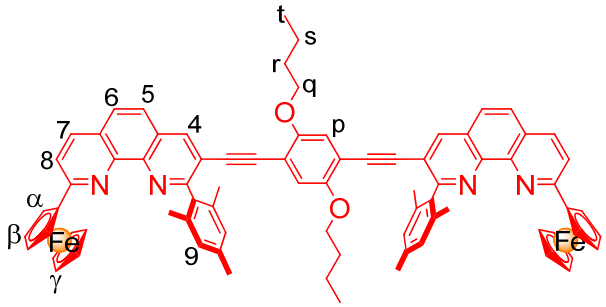

1

An oven-dried flask was charged with 1,4-dibutoxy-2,5-diiodobenzene (**10**, 38.0 mg, 80.0 μmol), 3-ethynyl-2-mesityl-9-ferrocenyl-[1,10]-phenanthroline (**9**, 100 mg, 197 μmol) and $Pd(PPh_3)_4$ (9.00 mg, 7.85 μmol) under nitrogen atmosphere. After addition of dry DMF (30 mL) and Et_3N (40 mL), the solution was degassed thrice by freeze-pump-thaw cycles. Finally the mixture was heated at 80 °C for 12 h under nitrogen atmosphere. The reaction mixture was then cooled down to room temperature and the solvents were removed under reduced pressure. The residue was dissolved in DCM and washed with water (200 mL). After drying over Na_2SO_4, the solvent was evaporated to furnish the crude product. The crude product was purified using column chromatography (SiO_2, *n*-hexane: ethyl acetate = 88:12) to furnish an orange solid. Yield = 24 mg (10%); mp 152 °C; ^{1}H NMR (400 MHz, CD_2Cl_2) δ = 8.45 (s, 2 H, 4-H), 8.17 (d, ^3J = 8.4 Hz, 2 H, 7-H), 7.82 (d, ^3J = 8.8 Hz, 2 H, 5-H), 7.82 (d, ^3J = 8.4 Hz, 2 H, 8-H), 7.79 (d, ^3J = 8.8 Hz, 2 H, 6-H), 7.07 (s, 4 H, 9-H), 6.42 (s, 2 H, p-H), 5.15 (t, ^3J = 2.0 Hz, 4 H, α-H), 4.48 (t, ^3J = 2.0 Hz, 4 H, β-H), 4.06 (s, 10 H, γ-H), 3.89 (t, ^3J = 6.4 Hz, 4 H, q-H), 2.42 (s, 6 H, Me-H), 2.14 (s, 12 H, Me-H), 1.85-1.78 (m, 4 H, r-H), 1.62-1.55 (m, 4 H, s-H), 1.08 (t, ^3J = 7.2 Hz, 6 H, t-H); ^{13}C NMR (100 MHz, CD_2Cl_2): δ = 161.3, 160.4, 153.4, 146.3, 145.0, 139.1, 137.9, 137.8, 136.8, 136.0, 128.4, 127.9, 127.6, 127.6, 125.0, 121.6, 120.0, 117.6, 114.1, 92.6, 91.7, 84.7, 70.8, 70.1, 69.5, 68.8, 31.7, 21.5, 20.2, 19.8, 14.2; IR (KBr) ν 3429, 2953, 2920, 2865, 2205, 1714, 1611, 1582, 1503, 1464, 1381, 1208, 1106, 1063, 1023, 846, 720, 638, 608, 484; ESI-MS: *m/z* (%) 1231.5 (100) $[M + H]^+$; Anal calcd for $C_{80}H_{70}N_4O_2Fe_2 \cdot H_2O$: C, 76.92; H, 5.81; N, 4.49; found: C, 76.78; H, 5.64, N, 4.24.

Model complex C4 = [Cu(3)(6)](PF$_6$).

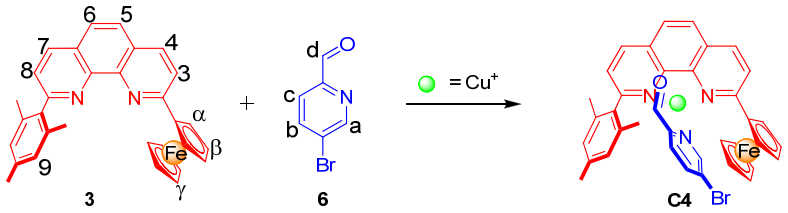

2-Ferrocenyl-9-mesityl-[1,10]-phenanthroline (**3**, 8.43 mg, 17.5 µmol), 5-bromopyridine-2-carboxaldehyde (**3**, 3.25 mg, 17.5 µmol) and [Cu(MeCN)$_4$]PF$_6$ (6.51 mg, 17.5 µmol) were placed in an NMR tube and dissolved in 500 µL of CD_2Cl_2. The resultant mixture was subjected to sonication for 1 h at 50°C. Then analytical characterisation was done without any purification. Yield: Quantative; mp (dec. > 180 °C); ^{1}H NMR (400 MHz, CD_2Cl_2): δ = 9.85 (s, 1 H, d-H), 8.63 (bs, 1 H, a-H), 8.62 (d, ^3J = 8.4 Hz, 1 H, 7-H), 8.46 (d, ^3J = 8.8 Hz, 1 H, 4-H), 8.24 (bd, ^3J = 8.4 Hz, 1 H, b-H), 8.18 (d, ^3J = 8.4 Hz, 1 H, 8-H), 8.06 (d, ^3J = 8.8 Hz, 1 H, [5/6] -H), 8.04 (d, ^3J = 8.8 Hz, 1 H, [6/5]-H), 7.83 (bd, ^3J = 8.4 Hz, 1 H, c-H), 7.80 (d, ^3J = 8.8 Hz, 1 H, 3-H), 6.76 (s, 2 H, 9-H), 5.03 (t, ^3J = 2.0 Hz, 2 H, α-H), 4.45 (t, ^3J = 2.0 Hz, 2 H, β-H), 4.14 (s, 5 H, γ-H), 2.26 (s, 3 H, Me), 1.92 (s, 6 H, Me); ^{13}C NMR (100 MHz, CD_2Cl_2): δ = 191.0, 161.6, 160.0, 151.1, 148.3, 144.0, 143.6, 140.8, 139.4, 139.2, 137.9, 137.8, 136.9, 136.1, 134.9, 128.4, 128.3, 128.0, 127.3, 126.8, 126.2, 126.0, 117.0, 72.3, 71.2, 69.7, 21.2, 20.3; IR (KBr) *v* 3447, 3088, 2917, 2857, 2373, 1614, 1583, 1511, 1355, 1280, 1108, 847, 556, 490; ESI-MS: *m/z* (%) 731.6 (100) $[M-PF_6]^+$; Anal calcd for $C_{37}H_{30}CuF_6FeN_3OPBr•1.5CH_2Cl_2•CH_3CN$: C, 46.53; H, 3.47; N, 5.36; found: C, 46.80; H, 3.13; N, 4.98.

Square S = $[Cu_4(1)_4](PF_6)_4$

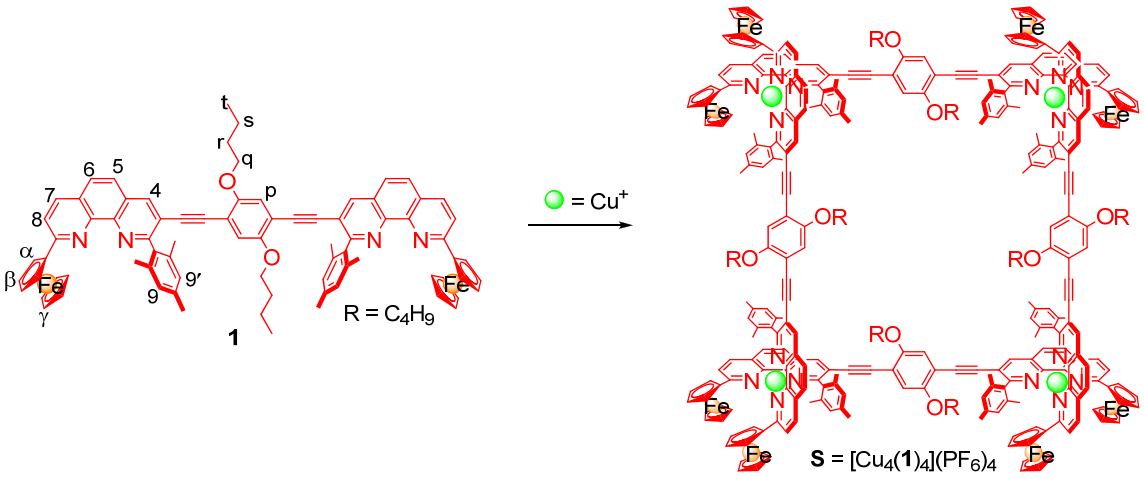

$[Cu(MeCN)_4]PF_6$ (405 μg, 1.08 μmol) and 9-(ferrocenyl)-3-((2,5-dibutoxy-4-((9-(ferrocenyl)-2-mesityl-1,10-phenanthrolin-3-yl)ethynyl)phenyl)ethynyl)-2-mesityl-1,10-phenanthroline (**1**, 1.33 mg, 1.08 μmol) were placed in a 25 mL flask and refluxed in 15 mL of CH_2Cl_2 for 30 min. After removal of the solvent under reduced pressure the resultant mixture was subjected to analytical characterisation without purification. Yield: Quantitative; ^{1}H NMR (400 MHz, 298 K, CD_2Cl_2): The square assembly **S** has four stereogenic cornerstones of the type $[Cu(\mathbf{1}_{phenAr2})(\mathbf{1}_{phenAr2})]^+$, so that four different diastereomeric may exist. Considering only the local symmetry of the individual stereogenic cornerstones, one would expect three different sets of ^{1}H NMR resonances for the $[Cu(\mathbf{1}_{phenAr2})(\mathbf{1}_{phenAr2})]^+$ motifs. Due to the overlap of resonances, it is not possible to determine the ratio of the diastereomers. Hence, we have characterised all protons collectively. δ = 8.55-8.41 (m, 8H, 4-H), 8.32-8.27 (m, 8H, 7-H), 8.06-7.91 (m, 24H, 5, 6 & 8-H), 6.43-6.29 (m, 8H, [9/9′]-H), 6.18-6.07 (m, 3H, p-H), 5.90-5.74 (m, 5H, p-H), 5.58-5.39 (m, 16H, [9′/9] & α-H), 5.02-4.96 (m, 8H, α-H), 4.57-4.53 (m, 8H, β-H), 4.29 (bs, 8H, β-H), 4.24 (s, 40H, γ-H), 3.53-3.50 (m, 16H, q-H), 2.07-2.01 (m, 24H, Me-H), 1.62-1.54 (m, 16H, r-H), 1.48-1.31 (m, 16H, s-H), 1.03-0.98 (m, 24H, Me-H), 0.96-0.85 (m, 24H, t-H), 0.73-0.63 (m, 24H, Me-H). ESI-MS: *m/z* (%) 1774.3 (100) $[M-PF_6]^{3+}$, 1294.5 (30) $[M]^{4+}$. Anal calcd for $C_{320}H_{280}Cu_4F_{24}Fe_8N_{16}O_8P_4 \cdot 5CH_2Cl_2$: C, 63.13; H, 4.73; N, 3.62; found: C, 62.91; H, 4.87; N, 3.33.

Triangle T = $[Cu_3(1)_2(2)](PF_6)_3$

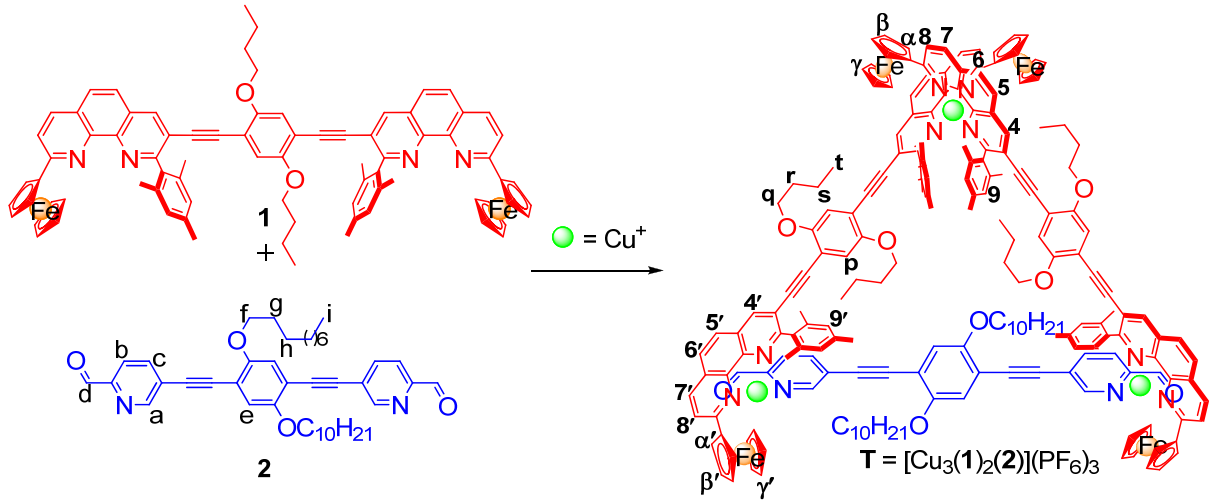

Ligand **1** (852 µg, 0.692 µmol), ligand **2** (224 µg, 0.345 µmol) and $[Cu(MeCN)_4]PF_6$ (387 µg, 1.02 µmol) were put in a 25 mL flask and dissolved in 15 mL of CH_3CN and CH_2Cl_2 (1:3). The resultant mixture was kept at reflux for 1 h. Thereafter, the solvent was removed under reduced pressure. The resultant mixture was subjected to analytical characterisation without purification. Yield: Quantitative; ^{1}H NMR (400 MHz, 298 K, CD_2Cl_2): δ = 9.77 (s, 0.88H, d-H), 9.74 (s, 1.12H, d-H), 8.67 (s, 0.88H, 4′-H), 8.62 (s, 1.12H, 4′-H), 8.51-8.39 (m, 6H, 4, 7′ & a-H), 8.34-8.28 (m, 2H, 7-H), 8.25-8.22 (m, 2H, b-H), 8.19-8.17 (m, 2H, 8′-H), 8.08-7.93 (m, 12H, 5, 6, 5′, 6′, 8 & c-H), 7.12 (s, 0.88H, e-H), 7.05 (s, 1.12H, e-H), 6.61 (s, 1.76H, 9′-H), 6.46-6.40 (m, 8.24H, p, 9 &9′-H), 5.62 (s, 0.88H, 9-H), 5.59 (s, 1.12H, 9-H), 5.58-5.52 (m, 2H, α-H), 5.02 (bs, 4H, α′-H), 4.98-4.95 (m, 2H, α-H), 4.57 (bs, 4H, β′-H), 4.34-4.30 (m, 2H, β-H), 4.26 (s, 4.4H, γ′-H), 4.25 (s, 5.6H, γ′-H), 4.13-4.11 (m, 12H, β & γ-H), 4.02 (t, ^3J = 6.8 Hz, 1.76H, f-H), 3.97 (t, ^3J = 6.8 Hz, 2.24H, f-H), 3.70 (t, ^3J = 6.4 Hz, 3.52H, q-H), 3.61 (t, ^3J = 6.4 Hz, 4.48H, q-H), 2.16-2.01 (m, 12H, Me-H), 1.83 (bs, 12H, Me-H), 1.77-1.70 (m, 4H, g-H),1.67-1.58 (m, 8H, r-H), 1.48-1.35 (m, 8H, s-H), 1.20-1.15 (m, 4H, h-H), 1.09-1.03 (m, 24H, -$(CH_2)_6$-H), 1.02-0.97 (m, 6H, Me-H), 0.96-0.92 (m, 12H, t-H), 0.89-0.86 (m, 2.64H, i-H), 0.83-0.78 (m, 3.36H, i-H), 0.69-0.65 (m, 6H, Me-H). From the integration ratio (e.g. aldehyde protons) we derived a ratio for the two diastereomers of 44:56. ESI-MS: *m/z* (%) 1722.7(100) $[M-PF_6]^{2+}$; Anal calcd for $C_{202}H_{192}Cu_3F_{18}Fe_4N_{10}O_8P_3$: C, 64.93; H, 5.18; N, 3.75; found: C, 65.37; H, 5.29; N, 3.61.

Rectangle R = $[Cu_4(10)_2(11)_2](PF_6)_4$

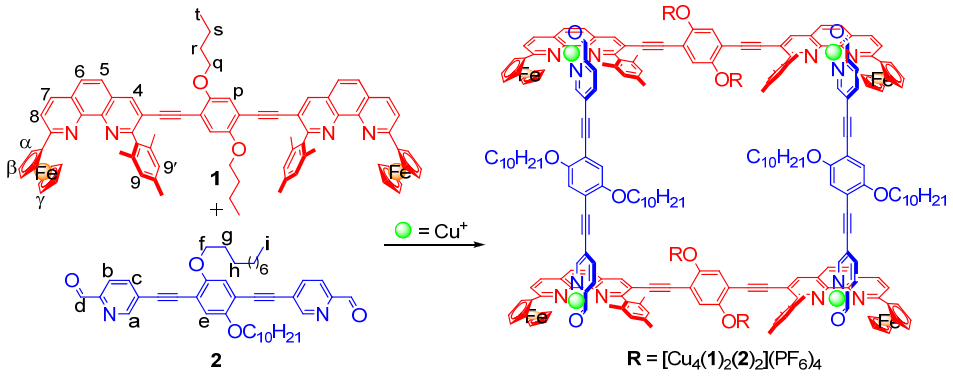

Ligand **1** (830 µg, 0.67 µmol), ligand **2** (437 µg, 0.67 µmol) and $[Cu(MeCN)_4]PF_6$ (503 µg, 1.35 µmol) were placed in a 25 mL round bottom flask and dissolved in 15 mL of CH_3CN and CH_2Cl_2 (1:4) mixture. The resultant mixture was subjected to reflux for 1 h, then the solvent was removed under reduced pressure.The resultant mixture was subjected to analytical characterisation without any purification. Yield quantitative; ^{1}H NMR (400 MHz, 298 K, CD_2Cl_2): δ = 9.80 (s, 4 H, d-H), 8.68 (s, 4 H, 4-H), 8.54 (bs, 4 H, a-H), 8.46 (d, ^3J = 8.8 Hz, 4H, 7-H), 8.20 (dd, ^3J = 8.8 Hz, ^4J = 1.6 Hz, 4H, b-H), 8.18 (d, ^3J = 8.8 Hz, 4H, 8-H), 8.06 (d, ^3J = 8.8 Hz, 4H, [5/6]-H), 8.02 (d, ^3J = 8.8 Hz, 4H, [6/5]-H), 7.94 (d, ^3J = 8.8 Hz, 4H, c-H), 7.07 (s, 4H, e-H), 6.62 (s, 8H, 9-H), 6.27 (s, 4H, p-H), 5.01 (t, ^3J = 1.6 Hz, 8H, α-H), 4.38 (t, ^3J = 1.6 Hz, 8H, β-H), 4.12 (s, 20H, γ-H), 4.00 (t, ^3J = 6.4 Hz, 8H, f-H), 3.73 (t, ^3J = 6.4 Hz, 8H, q-H), 2.20 (s, 12H, Me-H), 1.89 (s, 24H, Me-H), 1.81-1.72 (m, 8H, g-H), 1.71-1.63 (m, 8H, r-H), 1.52-1.39 (m, 16H, s, h-H), 1.25-1.06 (m, 48H, -$(CH_2)_6$-H), 0.99 (t, ^3J = 7.6 Hz, 12H, t-H), 0.82 (t, ^3J = 7.2 Hz, 12H, i-H). ESI-MS: *m/z* (%) 1003.5(100) $[M-PF_6]^{4+}$, 1385.6(30) $[M-PF_6]^{3+}$; Anal calcd for $C_{244}H_{244}Cu_4F_{24}Fe_4N_{12}O_{12}P_4$•$2CH_2Cl_2$: C, 62.02; H, 5.25; N, 3.53; found: C, 62.22; H, 5.19; N, 3.42.

Cyclic Interconversion experiments of the metallosupramolecular Architectures

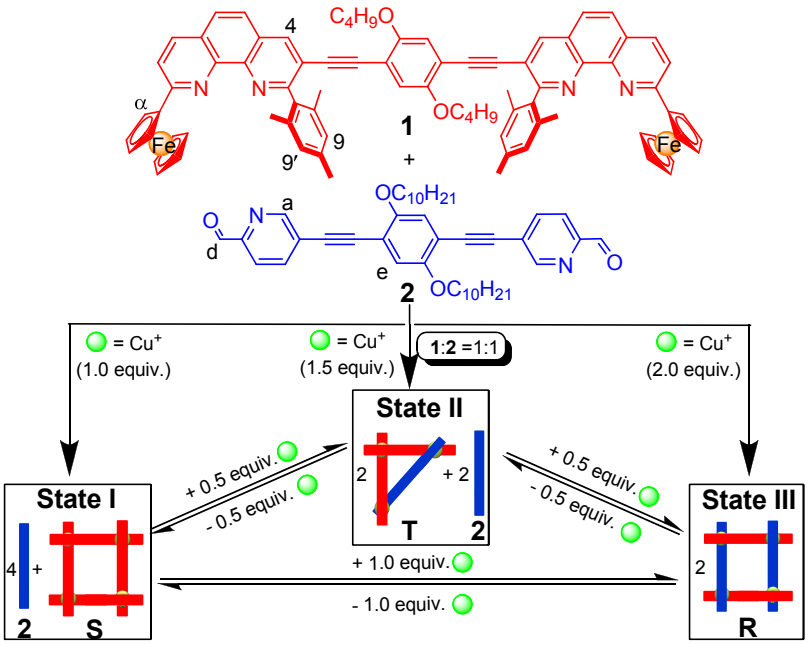

Scheme S1: Three-state cyclic interconversion of the metallosupramolecular complexes **S**, **T** and **R** depending on the Cu^{+} amount (equiv. refer to the amount of **1**).

Preparation of State I (S+2):

To prepare state I, ligand **1** (650 µg, 0.528 µmol), ligand **2** (343 µg, 0.528 µmol) and $[Cu(CH_3CN)_4]PF_6$ (197 µg, 0.528 µmol) were loaded in an oven dried 25 mL flask and subjected to relux for 1 h in 15 mL of CH_2Cl_2/CH_3CN (4:1). Thereafter, the solvents were removed under reduced pressure. Without any further purification the resultant solid was analysed by ^1H NMR and DOSY NMR (Figures S19 & S28).

Preparation of State II (T+2):

To prepare state II, ligand **1** (974 µg, 0.791 µmol), ligand **2** (513 µg, 0.791 µmol) and $[Cu(MeCN)_4]PF_6$ (442 µg, 1.18 µmol) were loaded in an oven dried 25 mL flask and subjected to relux for 1 h in 15 mL of CH_2Cl_2/CH_3CN (4:1). Thereafter, the solvents were removed under reduced pressure. Without any further purification the resultant solid was analysed by ^1H NMR and DOSY NMR (Figures S21& S29).

***In-situ* interconversion of all three states (see Scheme S1 and Figure S23):**

State I: Ligand **1** (2.65 mg, 2.15 μmol) and ligand **2** (1.40 mg, 2.15 μmol) were taken in a 25 mL flask and dissolved in 15 mL of CH_2Cl_2/CH_3CN (4:1 ratio) mixture. After addition of $[Cu(CH_3CN)_4]PF_6$ (819 μg, 2.15 μmol), the resultant red solution was refluxed for 1 h. Then the solvents were evaporated to dryness. The red solid was dissolved in CD_2Cl_2 and a portion of the resultant solution was subjected to ^1H NMR analysis (Figure S23(a)). **State II:** Subsequently, the NMR solution was quantitatively transferred back to the original flask and $[Cu(CH_3CN)_4]PF_6$ (410 μg, 1.07 μmol) as well as 15 mL of DCM were added. Then the resultant solution was refluxed for 1 h and the solvents were removed under reduced pressure. The solid was subjected to ^1H NMR analysis (Figure S23(b)). **State III:** After the NMR measurement the solution was again quantitatively transferred back into the original flask and $[Cu(CH_3CN)_4]PF_6$ (410 μg, 1.07 μmol) was added. The mixture was then refluxed for 1 h in 15 mL of CH_2Cl_2/CH_3CN (4:1). For analysis of the outcome, all solvents were removed under reduced pressure. Then, the product was investigated by ^1H NMR in CD_2Cl_2 (Figure S23(c)).

Reversibility of the cycle in scheme 1 (Figure S24):

To examine the reversibility of the cycle presented in scheme 1 we started from state III, i.e. from rectangle **R** (Figure S23(c)) prepared in above mentioned interconversion process. We used the full amount as obtained above in State III. **State II:** Cyclam (**8**, 216 μg, 1.07 μmol) was added and the mixture was refluxed for 1 h in 15 mL of CH_2Cl_2/CH_3CN (4:1). After removal of solvents under reduced pressure, the mixture was analysed by ^1H NMR (Figure S24(d)). **State I:** After the NMR measurement the sample was transferred back to the flask and cyclam (**8**, 216 μg, 1.07 μmol) was added to furnish state I (**S**+**2**) from state II (**T**+**2**). The mixture was subjected to reflux for 1 h in 15 mL of CH_2Cl_2/CH_3CN (4:1). Solvents were evaporated under reduced pressure and the mixture was analysed by ^1H NMR (Figure S24(e)).

^{1}H and ^{13}C NMR Spectra

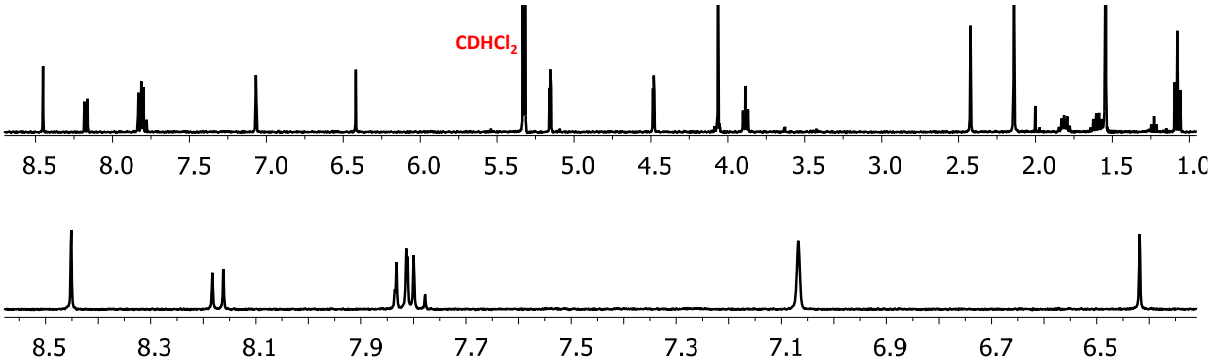

Figure S1: Full ^{1}H NMR spectrum (400 MHz, CD_2Cl_2, 298 K) of ligand **1**. An expanded part of the aromatic region is shown at the bottom.

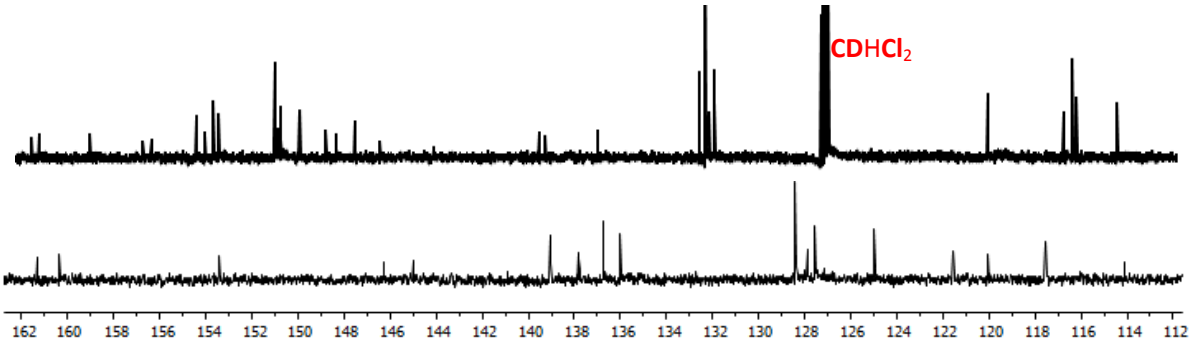

Figure S2: Full ^{13}C NMR spectrum (100 MHz, CD_2Cl_2, 298 K) of ligand **1**. An expanded part of the aromatic region is shown at the bottom.

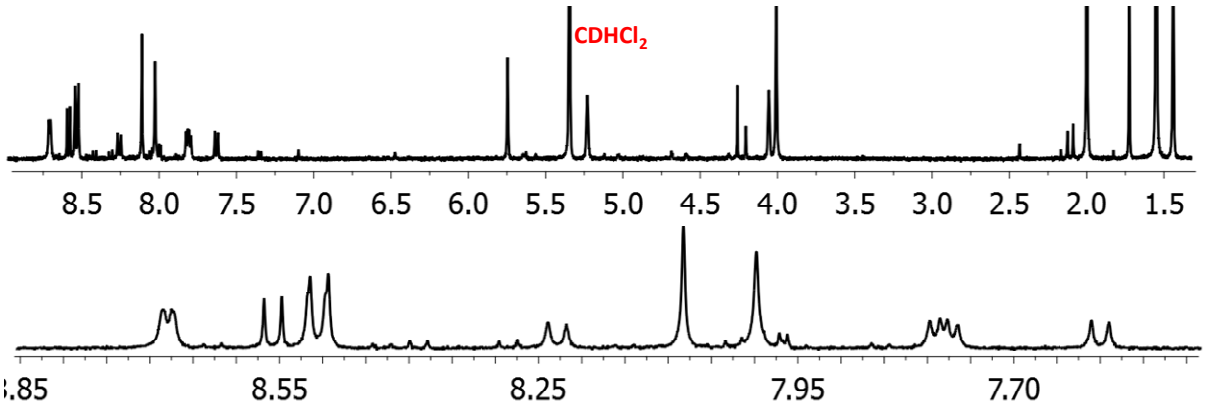

Figure S3: ^{1}H NMR spectrum (400 MHz, CD_2Cl_2, 298 K) of the mixture of ligand **3**, ligand **4** and $[Cu(CH_3CN)]PF_6$ in a 1:1:1 ratio. Complex **C2** = $[Cu(\mathbf{3})(\mathbf{4})]PF_6$ is the major product, but not formed quantitatively. An expanded part of the aromatic region is shown at the bottom.

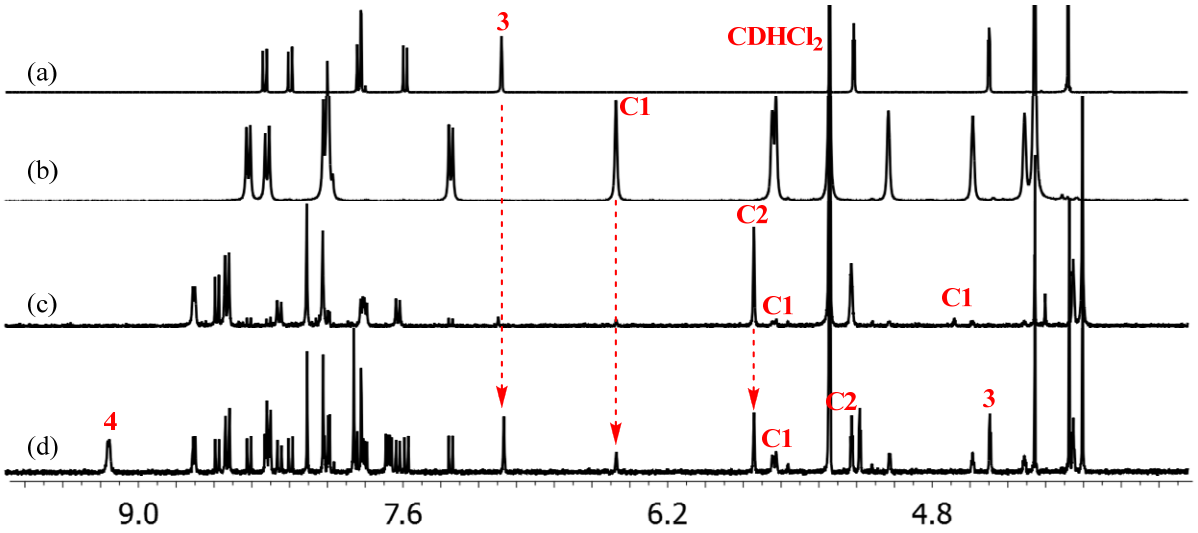

Figure S4: Partial ^{1}H NMR spectra for comparison (400 MHz, CD_2Cl_2, 298 K) of (a) ligand **3**, (b) **C1** = $[Cu(\mathbf{3})_2]PF_6$, (c) **C2** = $[Cu(\mathbf{3})(\mathbf{4})]PF_6$ (partial formation was observed from a 1:1:1 mixture of ligands **3**, **4** and $[Cu(CH_3CN)_4]PF_6$) and (d) a mixture of ligand **3**, ligand **4** and $[Cu(CH_3CN)_4]PF_6$ in 1:1:0.5 ratio.

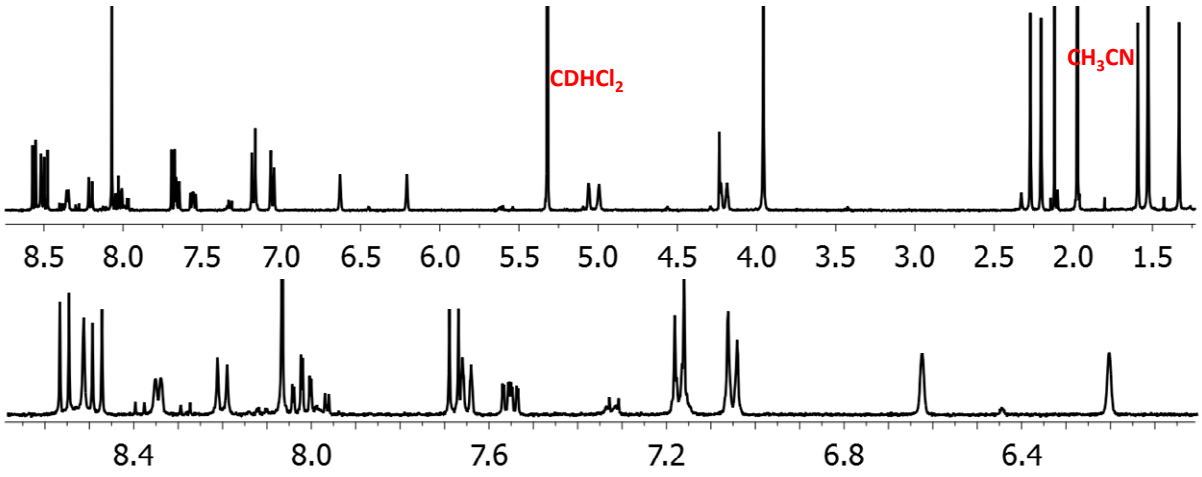

Figure S5: ^{1}H NMR spectrum (400 MHz, CD_2Cl_2, 298 K) of the mixture of ligand **3**, ligand **5** and $[Cu(CH_3CN)]PF_6$ in 1:1:1 ratio. Complex **C3** = $[Cu(\mathbf{3})(\mathbf{5})]PF_6$ is the major product, but not formed quantitatively. An expanded part of the aromatic region is shown at the bottom.

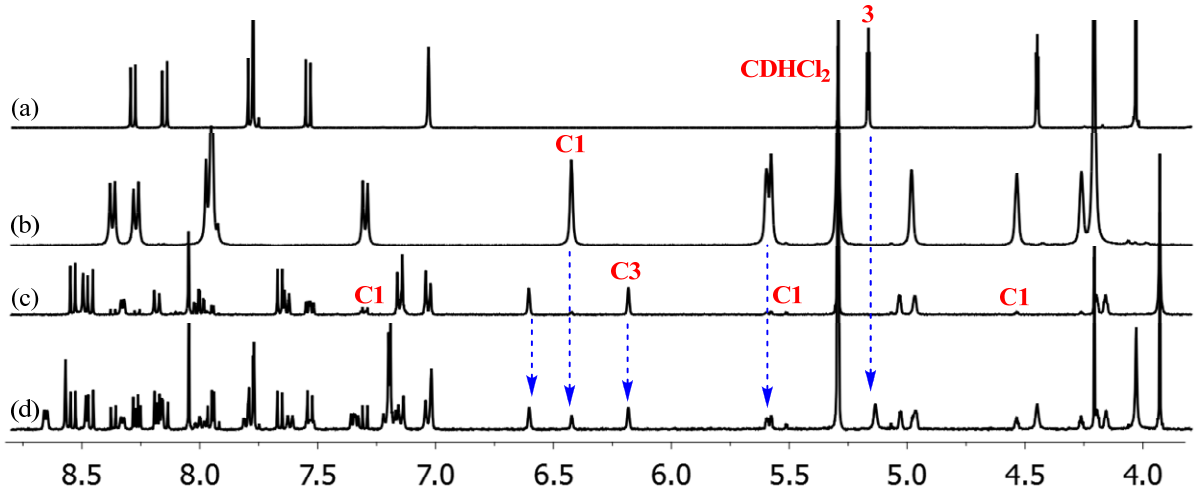

Figure S6 : Partial ^{1}H NMR spectra for comparison (400 MHz, CD_2Cl_2, 298 K) of (a) ligand **3**, (b) **C1** = $[Cu(\mathbf{3})_2]PF_6$, (c) **C3** = $[Cu(\mathbf{3})(\mathbf{5})]PF_6$ (partial formation was observed from a 1:1:1 mixture of ligands **3**, **4** and $[Cu(CH_3CN)_4]PF_6$), and (d) a mixture of ligand **3**, ligand **5** and $[Cu(CH_3CN)_4]PF_6$ in 1:1:0.5 ratio.

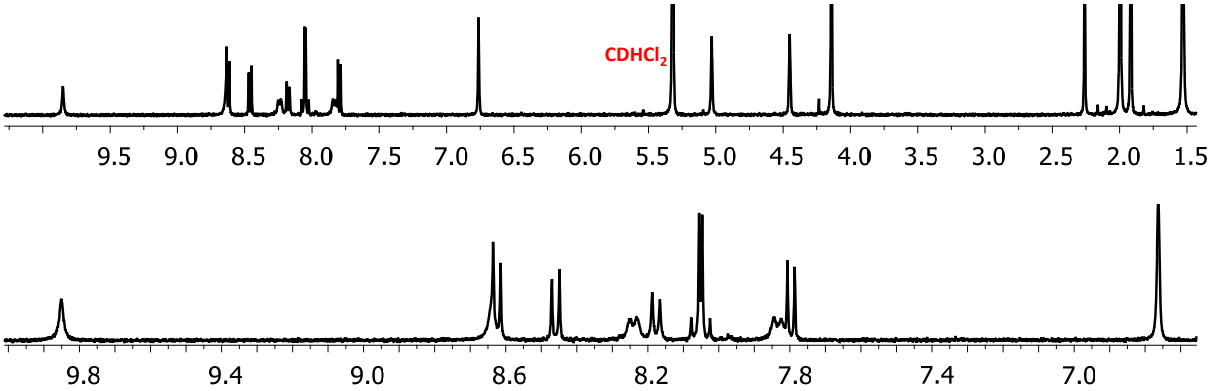

Figure S7: ^{1}H NMR spectrum (400 MHz, CD_2Cl_2, 298 K) of complex **C4** = $[Cu(\mathbf{3})(\mathbf{6})]PF_6$. An expanded part of the aromatic region is shown at the bottom.

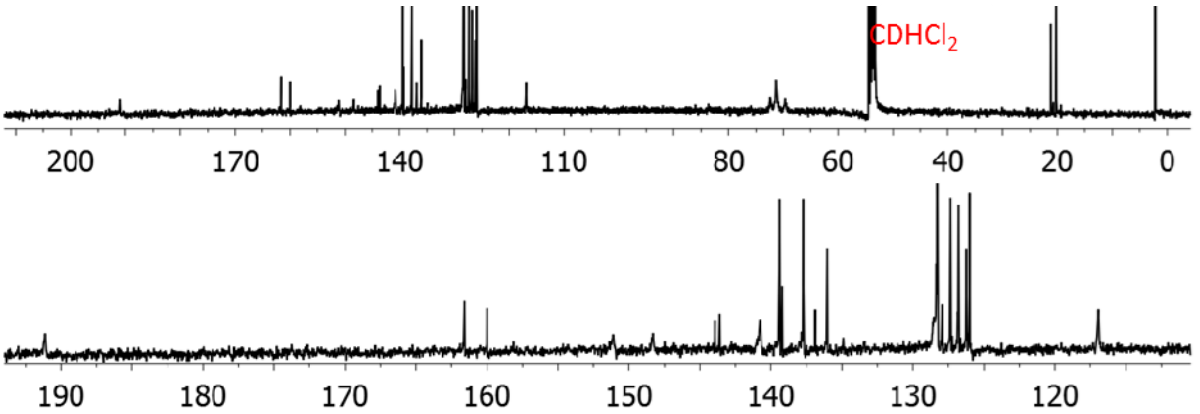

Figure S8 : ^{13}C NMR spectrum (100 MHz, CD_2Cl_2, 298 K) of complex **C4** = $[Cu(\mathbf{3})(\mathbf{6})]PF_6$. An expanded part of the aromatic region is shown at the bottom.

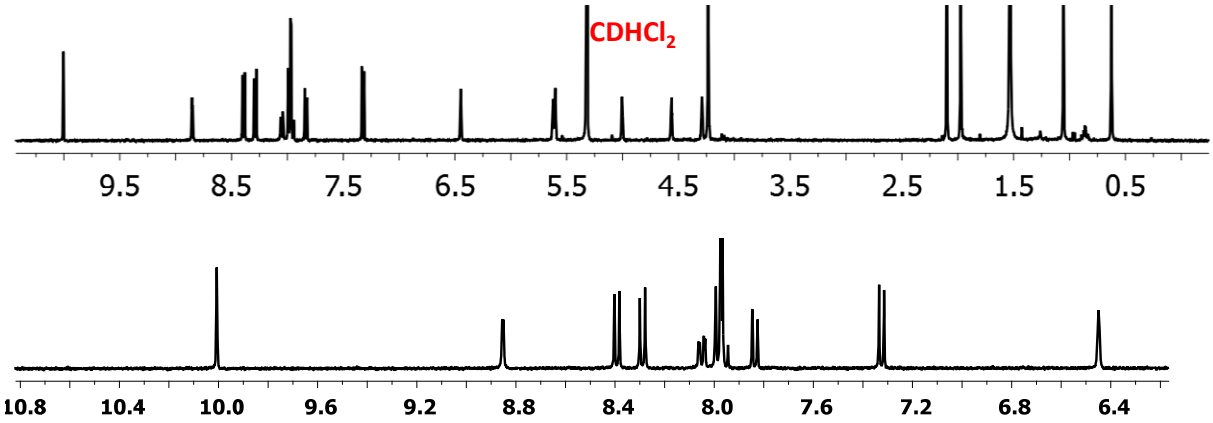

Figure S9: ^{1}H NMR spectrum (400 MHz, CD_2Cl_2, 298 K) of ligand **3**, ligand **6** and $[Cu(CH_3CN)_4]PF_6$ in 2:2:1 ratio (state I', Scheme 2 as described in the manuscript). An expanded part of the aromatic region is shown at the bottom.

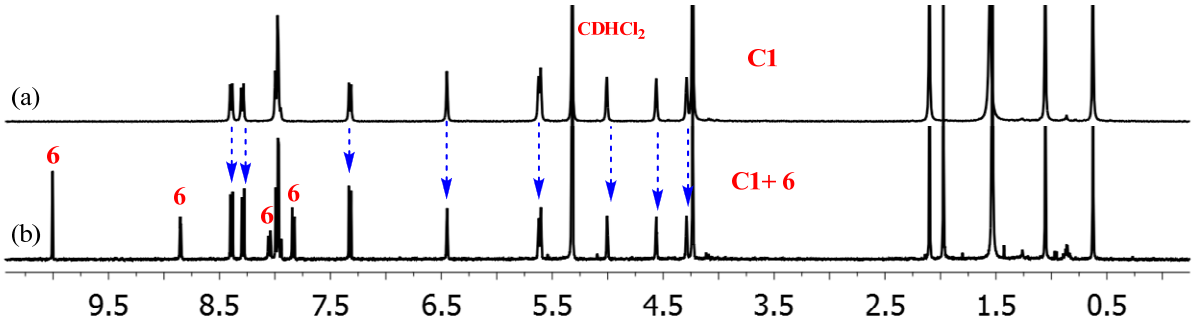

Figure S10: Partial ^{1}H NMR (400 MHz, CD_2Cl_2, 298 K) spectra for comparison of: (a) **C1**= $[Cu(\mathbf{3})_2]PF_6$, (b) a mixture of ligand **3**, ligand **6** and $[Cu(CH_3CN)_4]PF_6$ in 2:2:1 ratio, representing state I' of Scheme 2 (see manuscript).

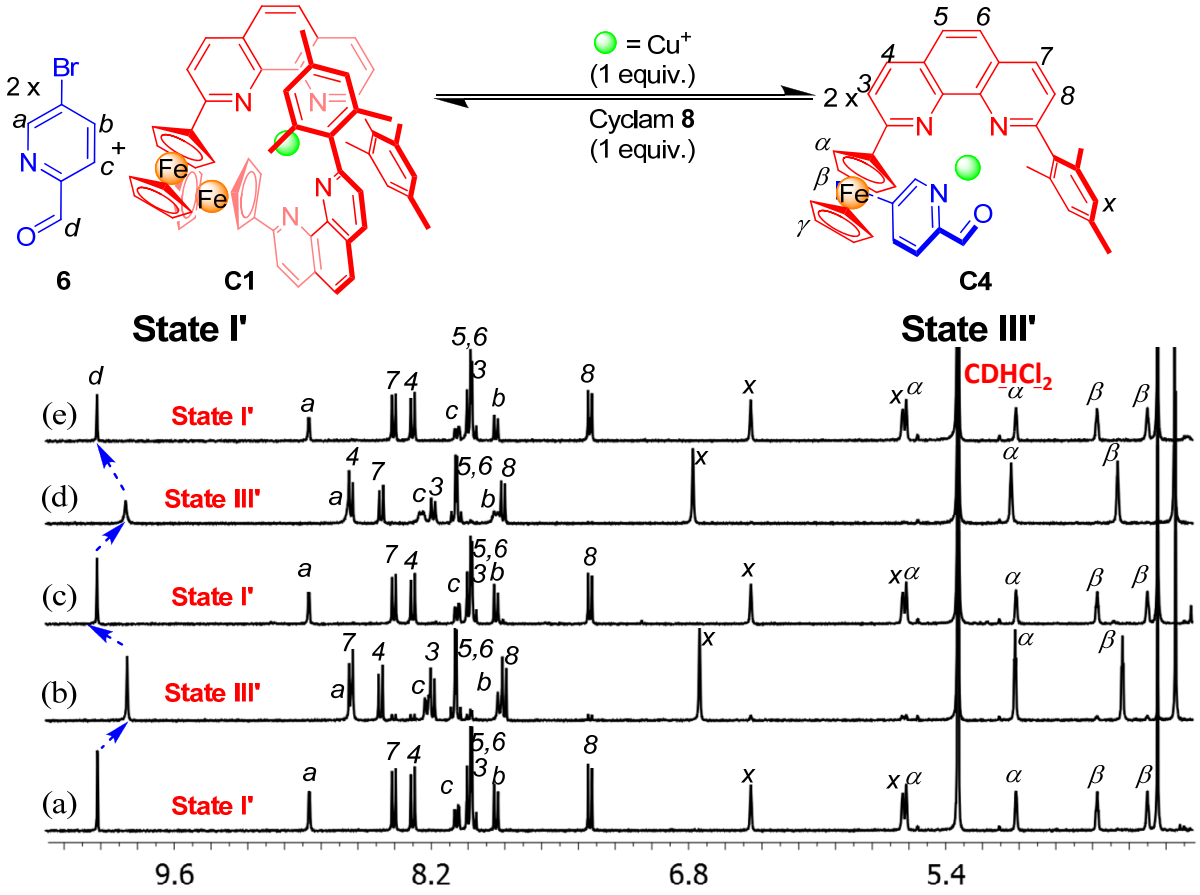

Figure S11: Partial ^{1}H NMR spectra (400 MHz, CD_2Cl_2, 298 K) depicting the reversible switching cycles between **C1** + **6** and **C4**. (a) (c) and (e) correspond to **C1** + **6** whereas (b) and (d) represent **C4**, obtained after successive addition of Cu^{+} (0.5 eq.) and cyclam (0.5 eq.) to a 1:1 mixture of ligands **3** and **6**.

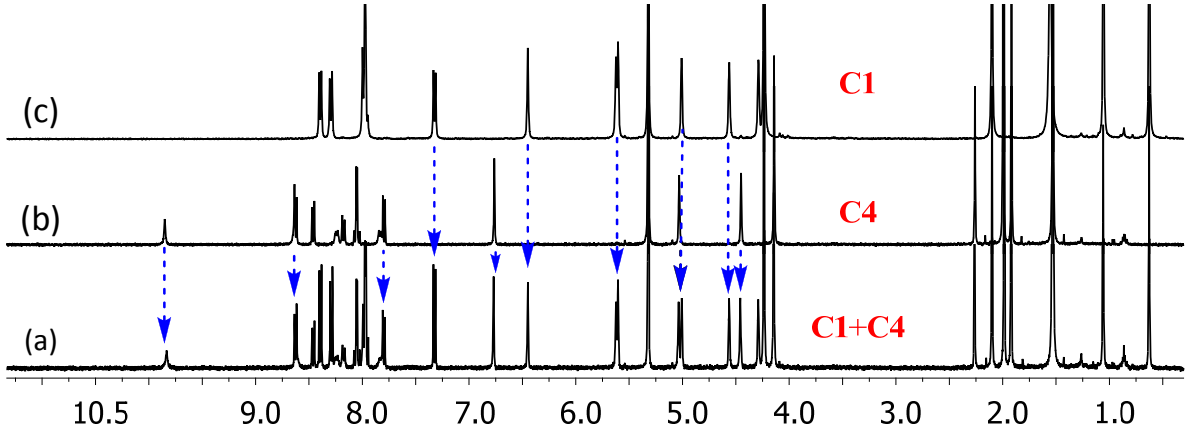

Figure S12: Partial ^{1}H NMR spectra (400 MHz, CD_2Cl_2, 298 K) of (a) a mixture of ligand **3**, ligand **6** and $[Cu(CH_3CN)_4]PF_6$ in 3:1:2 ratio, *i.e.* complexes **C1** and **C4** in a 1:1 ratio, (b) **C4** = $[Cu(\mathbf{3})(\mathbf{6})]PF_6$ and (c) **C1**= $[Cu(\mathbf{3})_2]PF_6$.

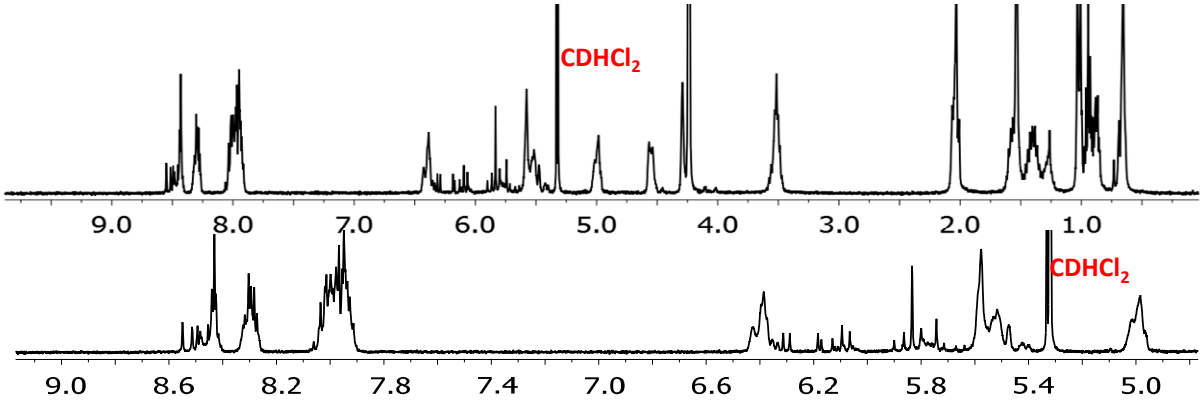

Figure S13: ^{1}H NMR spectrum (400 MHz, CD_2Cl_2, 298 K) of square **S** = $[Cu_4(\mathbf{1})_4](PF_6)_4$. An expanded part of the aromatic region is shown at the bottom.

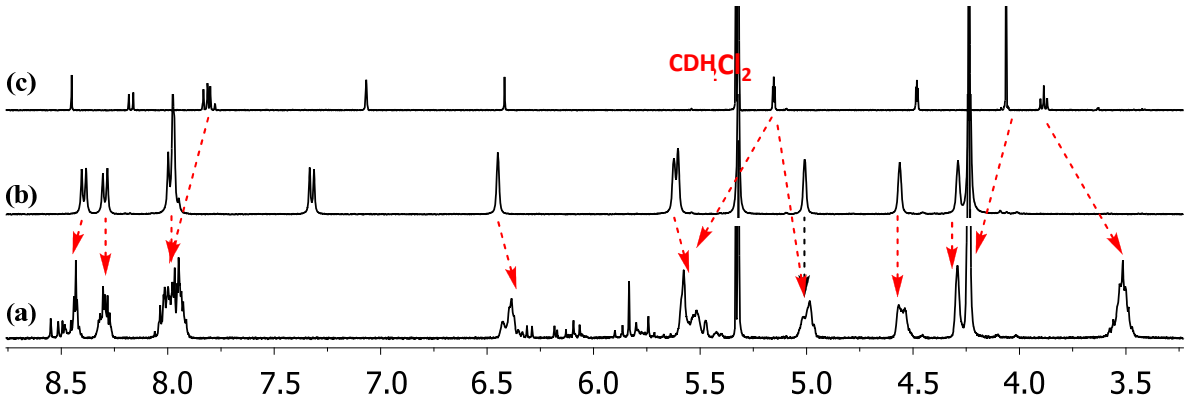

Figure S14: Partial ^{1}H NMR spectra (400 MHz, CD_2Cl_2, 298 K) of (c) ligand **1**, (b) **C1** = $[Cu(\mathbf{3})_2]PF_6$ and (a) square **S** = $[Cu_4(\mathbf{1})_4](PF_6)_4$.

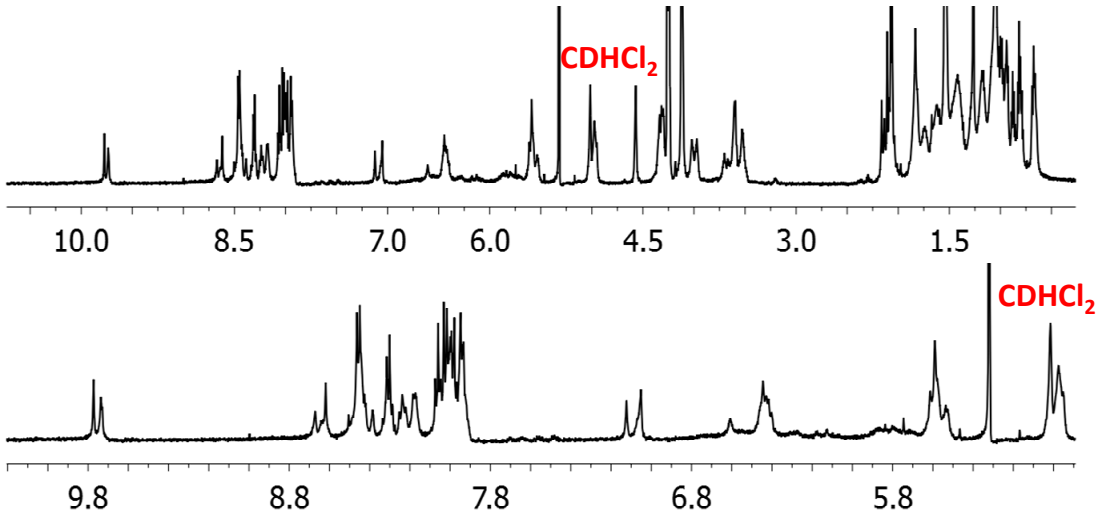

Figure S15: ^{1}H NMR spectrum (400 MHz, CD_2Cl_2, 298 K) of triangle **T** = $[Cu_3(\mathbf{1})_2(\mathbf{2})](PF_6)_3$. An expanded part of the aromatic region is shown at the bottom.

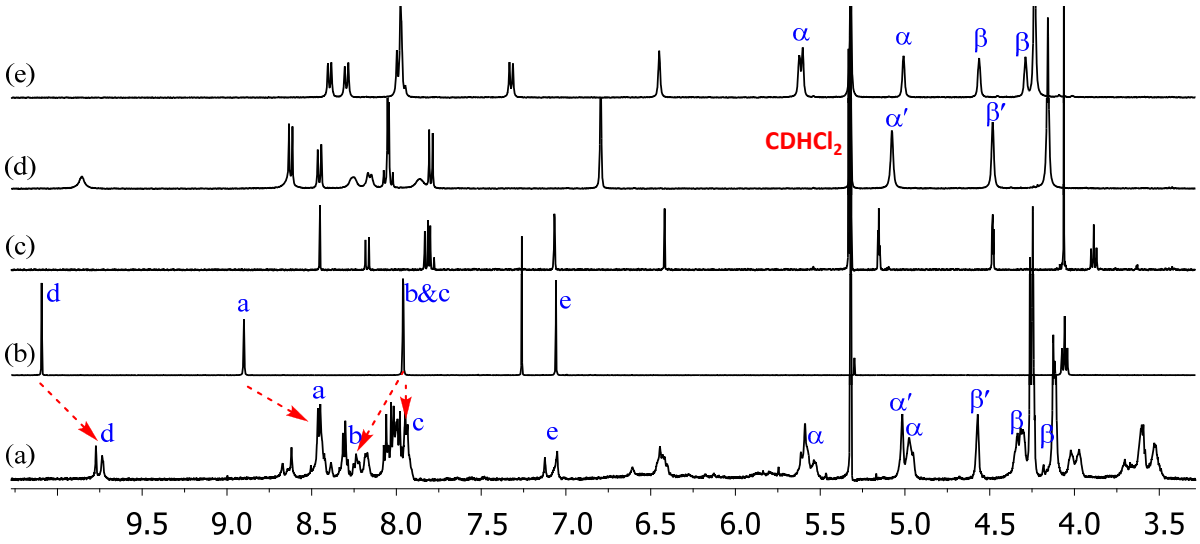

Figure S16: Partial ^{1}H NMR spectra (400 MHz, CD_2Cl_2, 298 K) of (e) **C1** = [Cu(**3**)$_2$]PF_6, (d) **C4** = [Cu(**3**)(**6**)]PF_6, (c) ligand **1**, (b) ligand **2**, and (a) triangle **T** = [Cu_3(**1**)$_2$(**2**)](PF_6)$_3$.

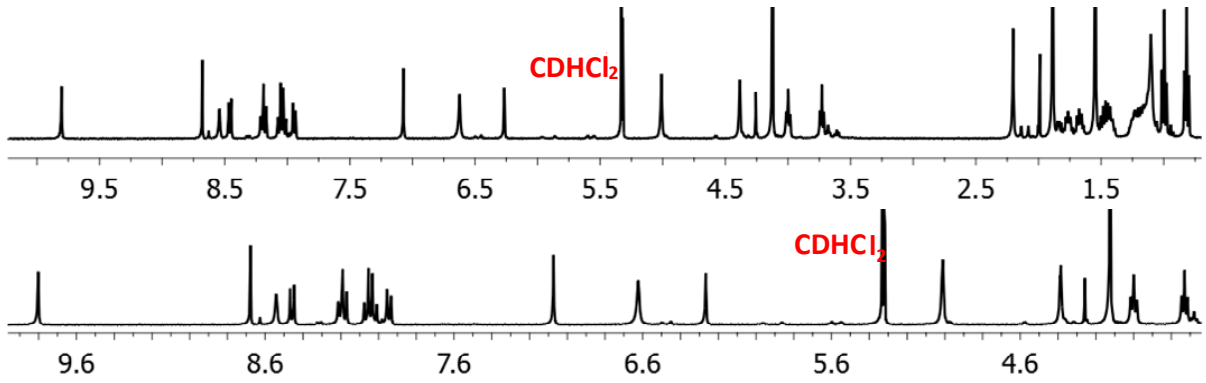

Figure S17: ^{1}H NMR spectrum (400 MHz, CD_2Cl_2, 298 K) of rectangle **R** = [Cu_4(**1**)$_2$(**2**)$_2$](PF_6)$_4$. An expanded part of the aromatic region is shown at the bottom.

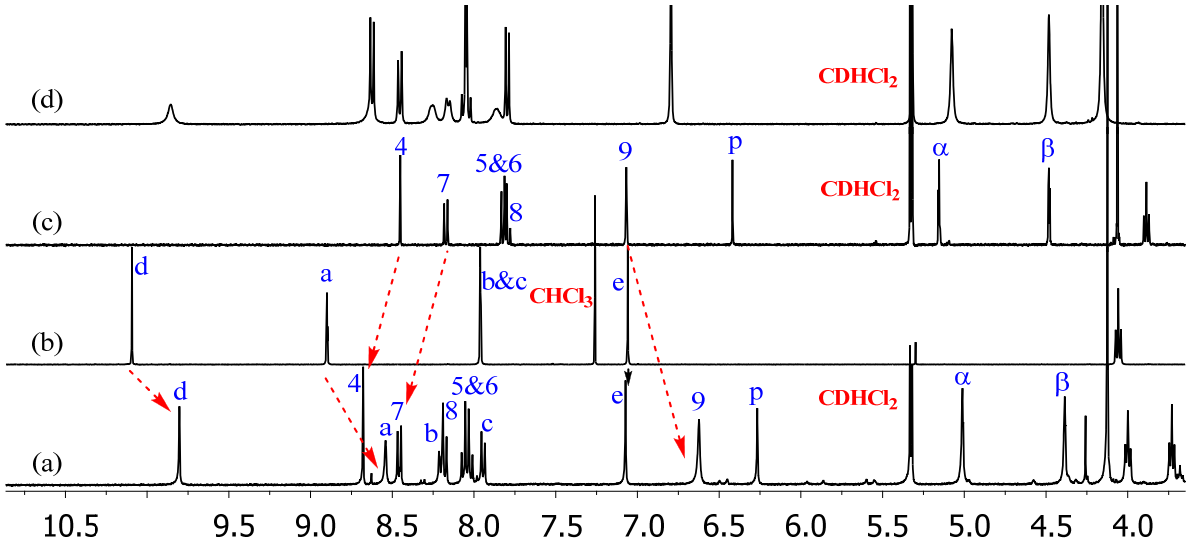

Figure S18: Partial ^{1}H NMR spectra (400 MHz, CD_2Cl_2, 298 K) of (d) **C4** = [Cu(**3**)(**6**)]PF_6, (c) ligand **1**, (b) ligand **2**, and (a) rectangle **R** = $[Cu_4(\mathbf{1})_2(\mathbf{2})_2](PF_6)_4$.

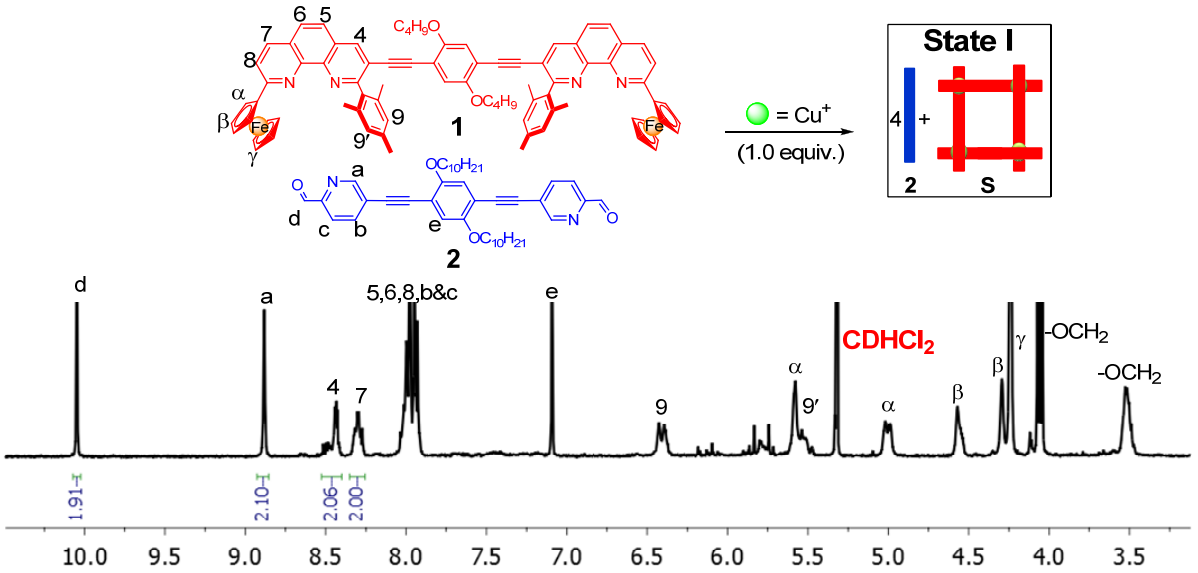

Figure S19: ^{1}H NMR spectrum (400 MHz, CD_2Cl_2, 298 K) of a mixture of ligand **1**, ligand **2** and $[Cu(CH_3CN)_4]PF_6$ in a 1:1:1 ratio after 1 h reflux , *i.e.* state I of Scheme S1. The spectrum shows **S** (1 eq.) = $[Cu_4(\mathbf{1})_4](PF_6)_4$ and ligand **2** (4 eq.).

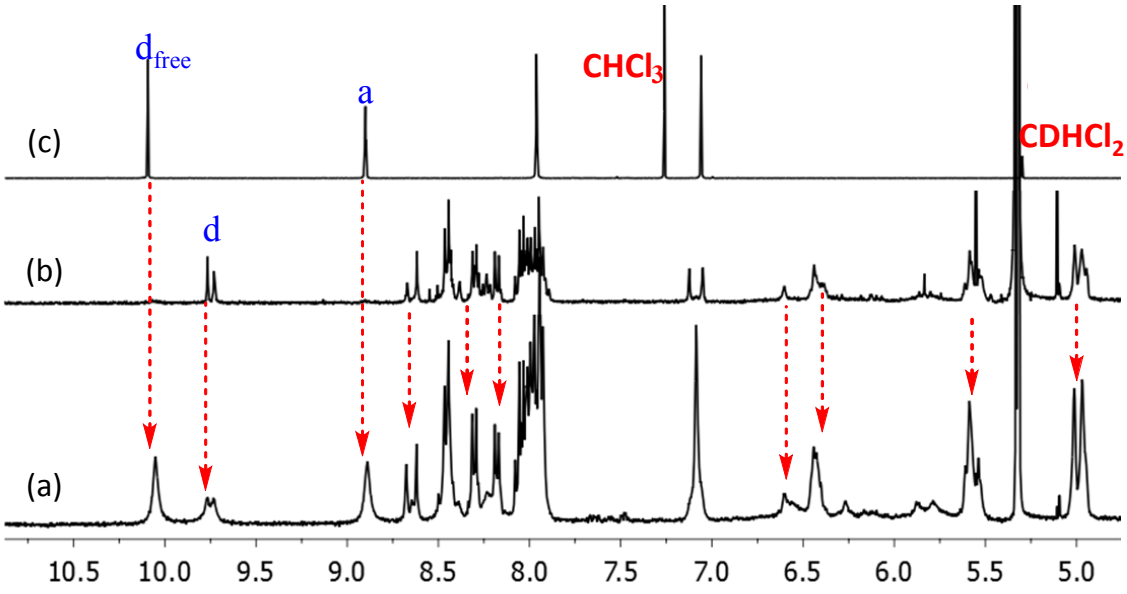

Figure S20: Partial ^{1}H NMR spectra for comparison (400 MHz, CD_2Cl_2, 298 K): of (c) ligand **2** , (b) square **S** = $[Cu_4(\mathbf{1})_4](PF_6)_4$, and (a) a mixture of ligand **1**, ligand **2** and $[Cu(CH_3CN)_4]PF_6$ in a 1:1:1 ratio.

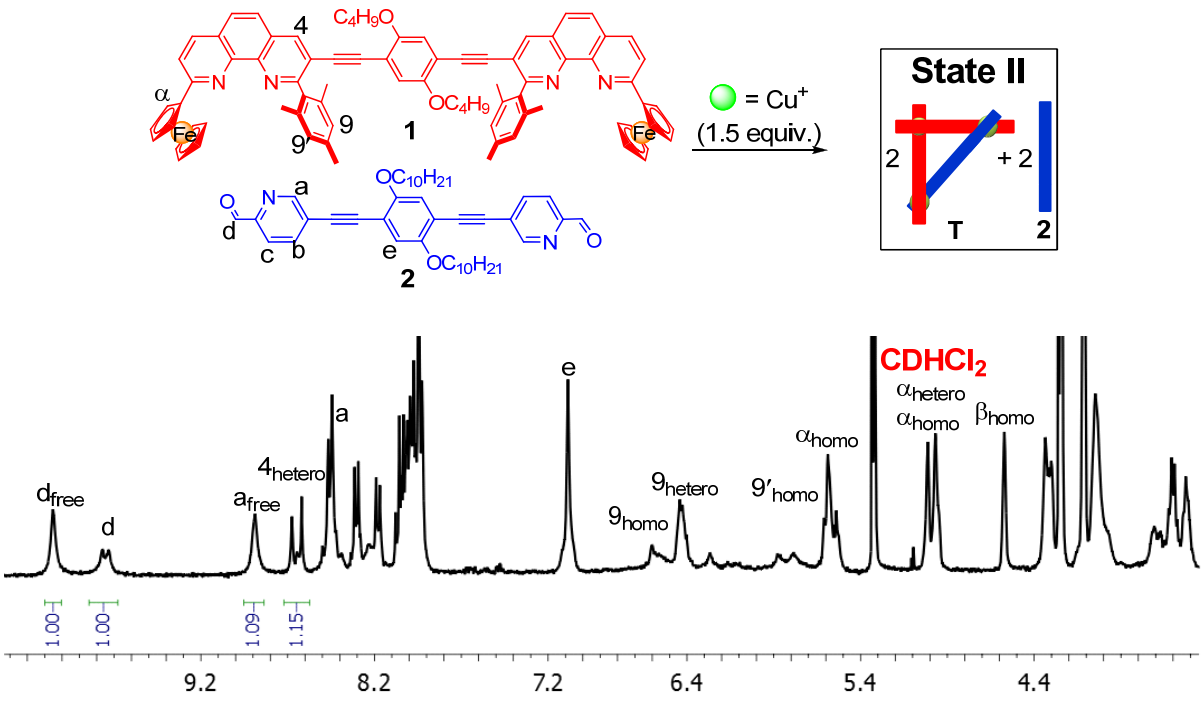

Figure S21: ^{1}H NMR spectrum (400 MHz, CD_2Cl_2, 298 K) of ligand **1**, ligand **2** and $[Cu(CH_3CN)_4]PF_6$ in a 2:2:3 ratio after 1 h reflux, i.e. state II (Scheme S1) = **T** (0.5 eq.) = $[Cu_3(\mathbf{1})_2(\mathbf{2})](PF_6)_3$) and ligand **2** (0.5 eq.). Ligand **1** is engaged in homo- and heteroleptic complexation.

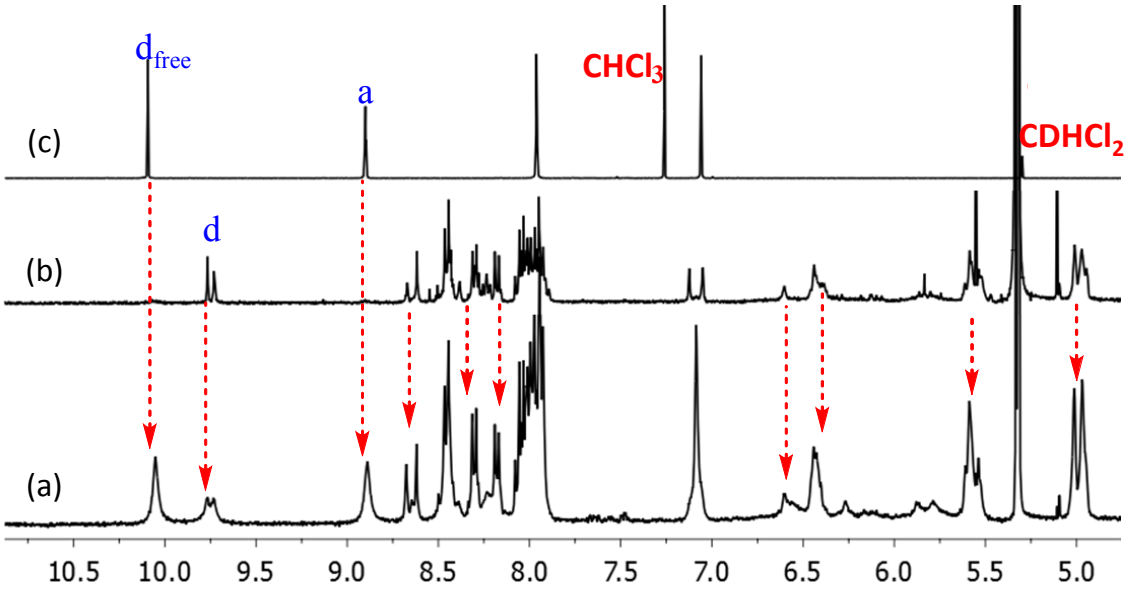

Figure S22: Partial ^{1}H NMR spectra (400 MHz, CD_2Cl_2, 298 K) of (c) ligand **2**, (b) triangle **T** = $[Cu_3(\mathbf{1})_2(\mathbf{2})](PF_6)_3$ and (a) a mixture of ligand **1**, ligand **2** and $[Cu(CH_3CN)_4]PF_6$ in 2:2:3 ratio after 1 h reflux.

^{1}H NMR for the Cyclic Interconversion experiments of the metallosupramolecular Architectures

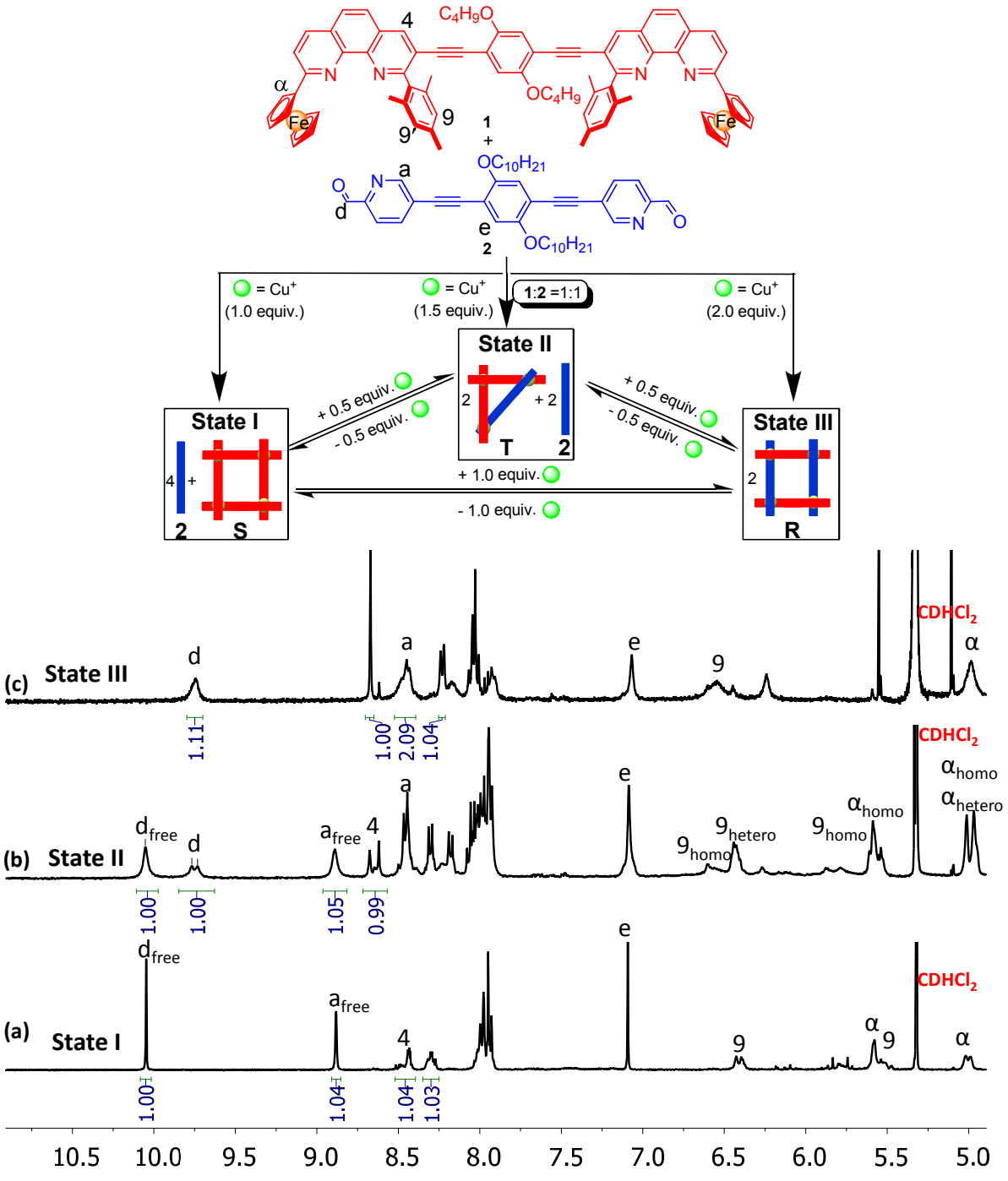

Figure S23: Partial ^{1}H NMR spectra for comparison (400 MHz, CD_2Cl_2, 298 K) of ligand **1** and ligand **2** in 1:1 ratio (a) with 1 eq. Cu^+; (b) with 1.5 eq. Cu^+; (c) with 2 eq. Cu^+. Ligand **1** is engaged in homo- and heteroleptic complexation.

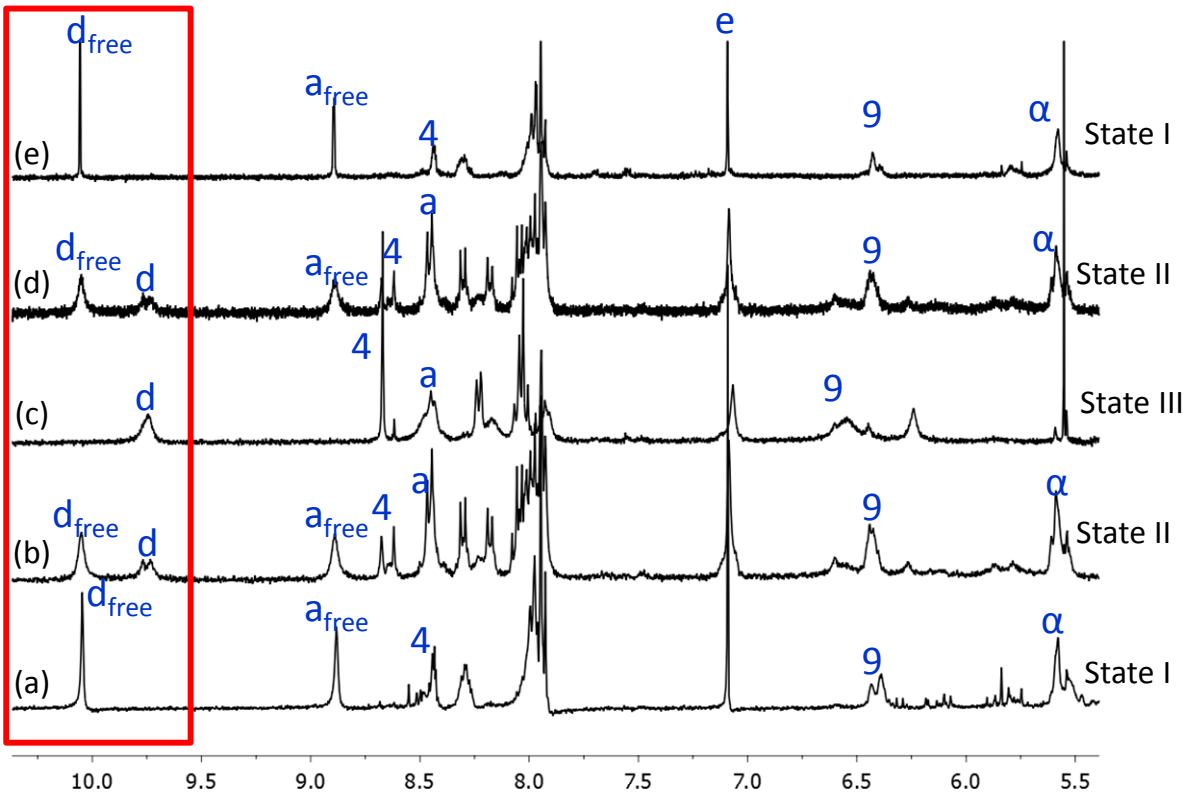

Figure S24: Partial ^{1}H NMR spectra (400 MHz, CD_2Cl_2, 298 K) that depict the reversibility of the cyclic interconversion. (a) Ligands **1** and **2** in 1:1 ratio after addition of 1 eq. Cu^{+}; (b) after addition of 0.5 eq. of Cu^{+} to (a); (c) after addition of 0.5 eq. of Cu^{+} to (b); (d) after addition of 0.5 eq. of cyclam (**8**) to (c); (e) after addition of 0.5 eq. of cyclam (**8**) to (d).

DOSY NMR

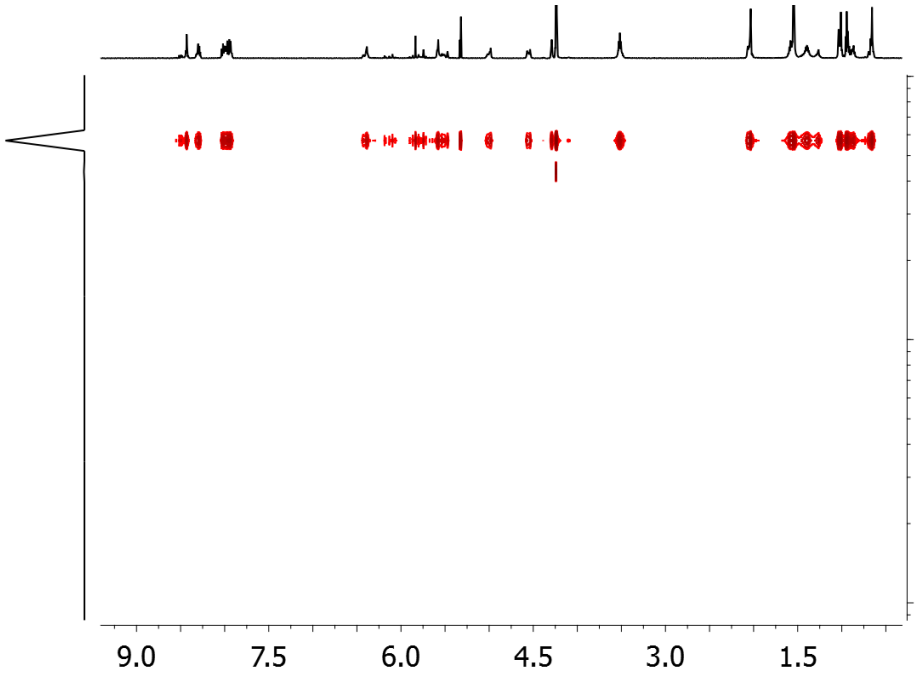

Figure S25: DOSY NMR spectrum (600 MHz, CD_2Cl_2, 298 K) of square **S** = $[Cu_4(\mathbf{1})_4](PF_6)_4$.

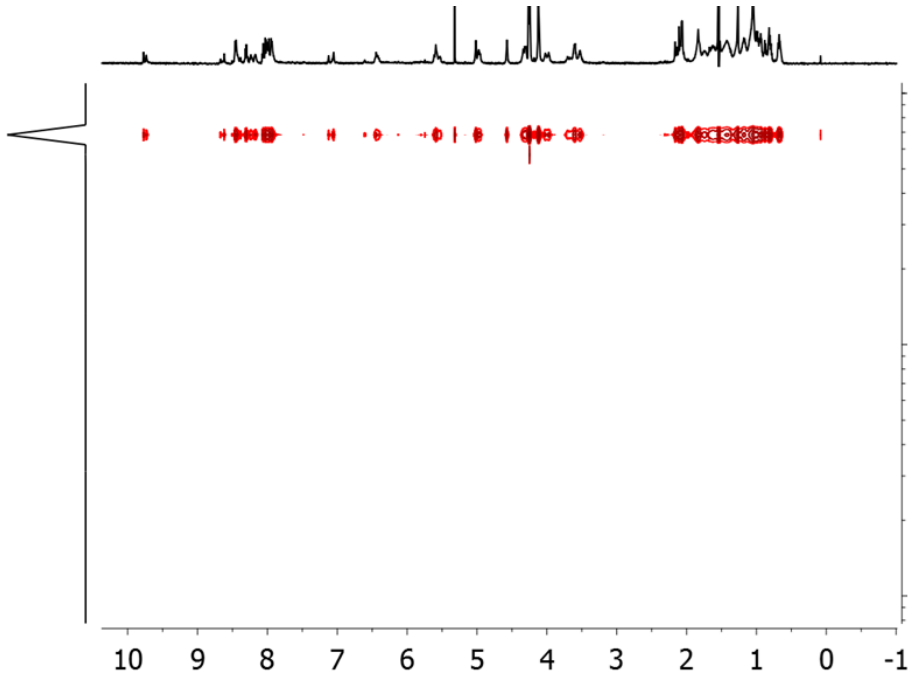

Figure S26: DOSY NMR spectrum (600 MHz, CD_2Cl_2, 298 K) of triangle **T** = $[Cu_3(\mathbf{1})_2(\mathbf{2})](PF_6)_3$.

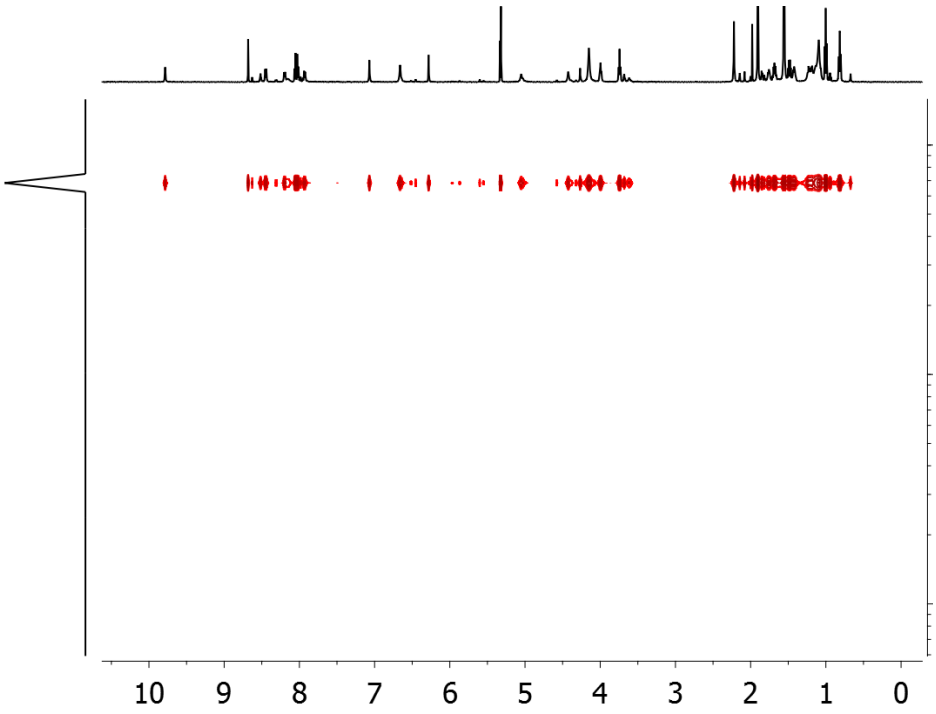

Figure S27: DOSY NMR spectrum (600 MHz, CD_2Cl_2, 298 K) of rectangle **R** = $[Cu_4(\mathbf{1})_2(\mathbf{2})_2](PF_6)_4$.

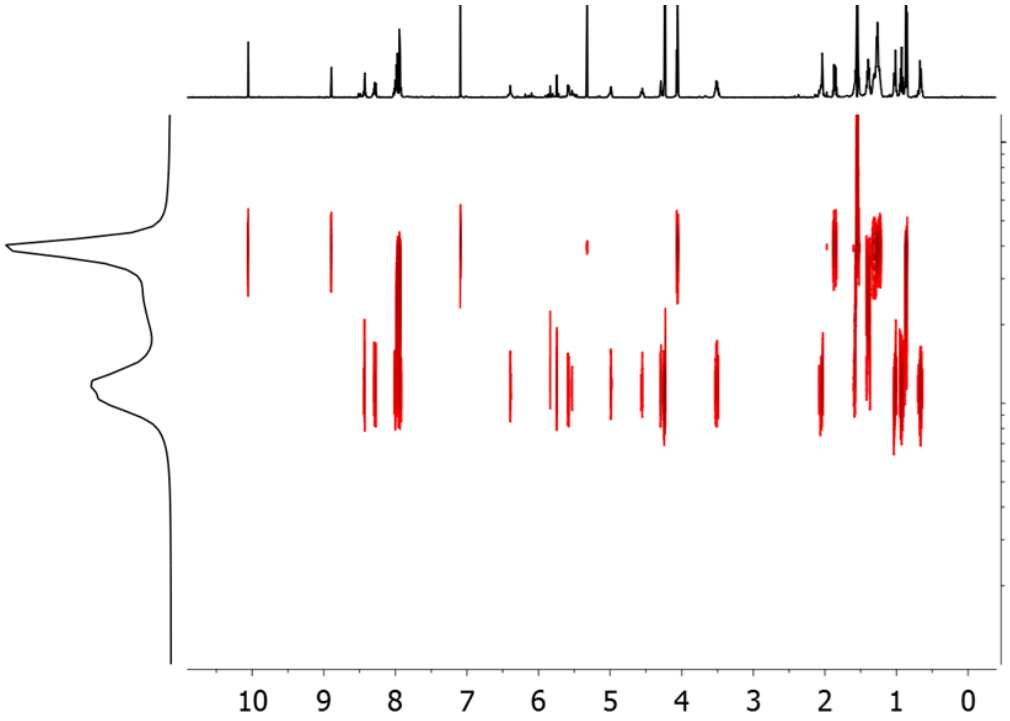

Figure S28: DOSY NMR spectrum (600 MHz, CD_2Cl_2, 298 K) of ligands **1** and **2** mixed with $[Cu(CH_3CN)_4]PF_6$ in a 1:1:1 ratio. The two separate diffusion line sets confirm the presence of two types of species in the mixture, i.e. state I = Square **S** and ligand **2** (see Scheme S1).

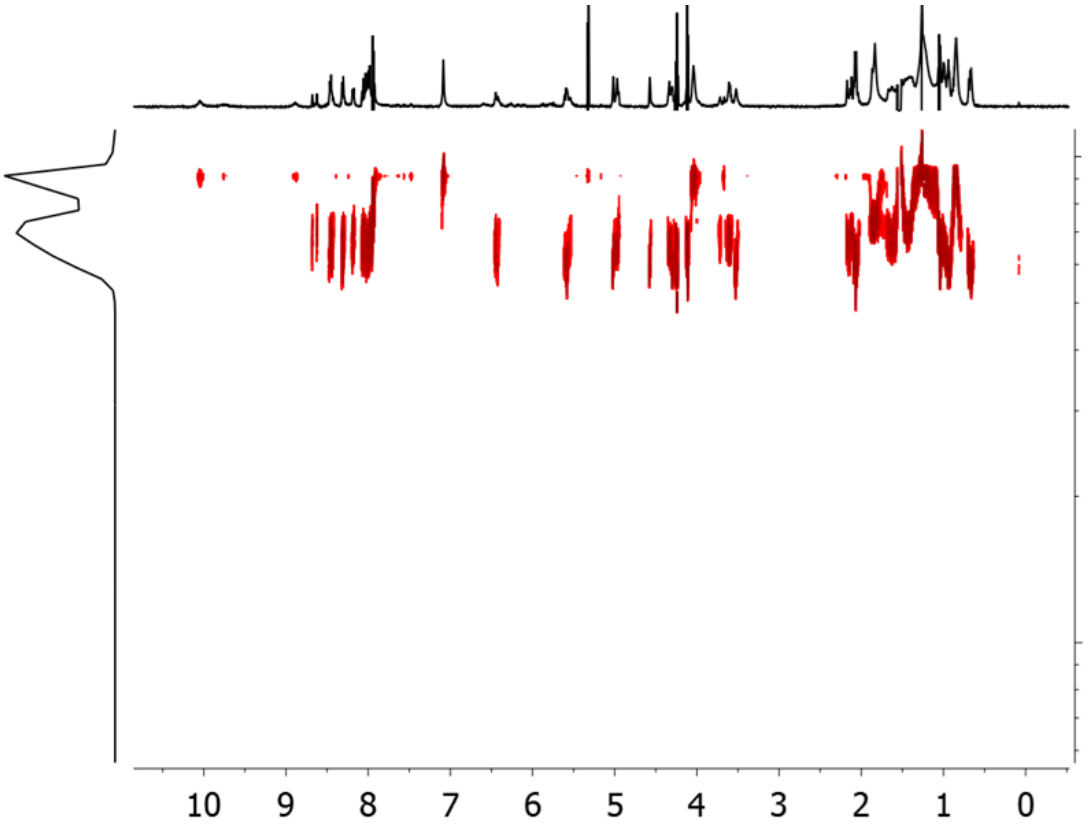

Figure S29: DOSY NMR Spectrum (600MHz, CD_2Cl_2, 298 K) of ligands **1** and **2** mixed with $[Cu(CH_3CN)_4]PF_6$ in 2:2:3 ratio. The two separate diffusion line sets confirm the presence of two types of species in the mixture, i.e. state II = triangle **T** and ligand **2** (Scheme S1).

ESI-MS:

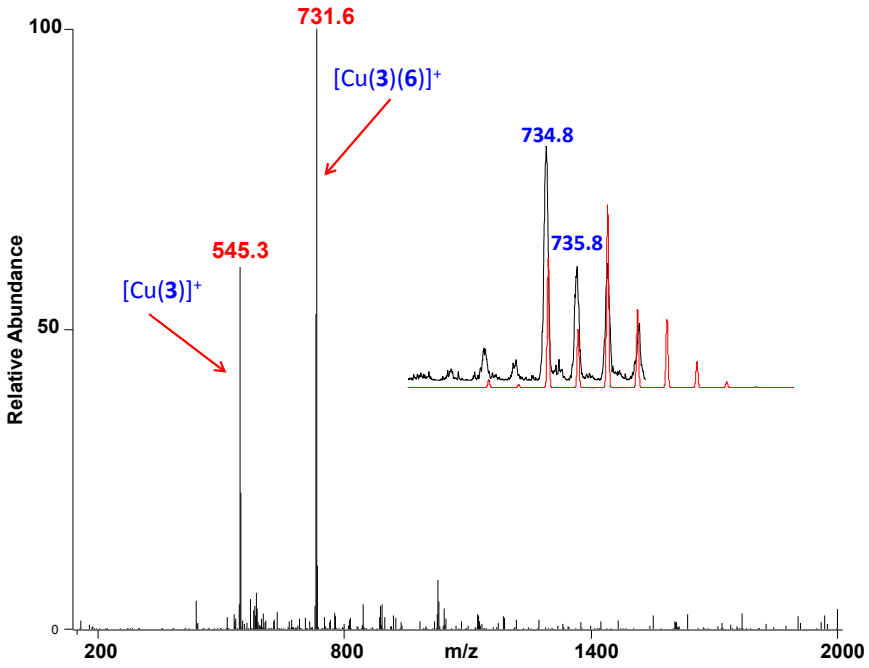

Figure S30: ESI-MS spectrum of complex **C4** = [Cu(**3**)(**6**)]PF_6 (in DCM) along with experimental (black) and calculated isotopic distributions (red) for the species [Cu(**3**)(**6**)]$^+$.

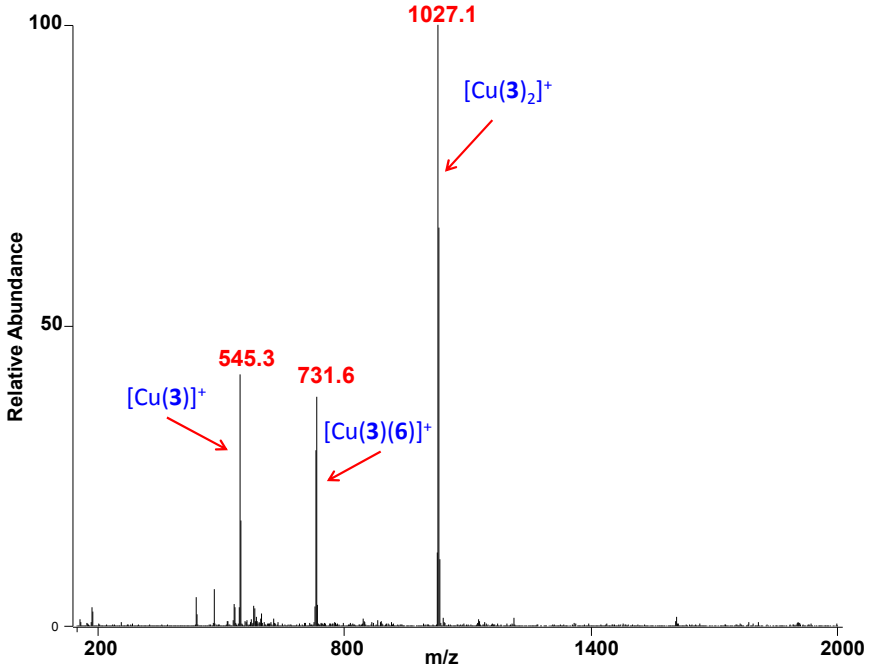

Figure S31: ESI-MS spectrum of an equimolar mixture of complexes **C1** and **C4** (in DCM). (**C1** = [Cu(**3**)$_2$]PF_6 and **C4**= [Cu(**3**)(**6**)]PF_6)

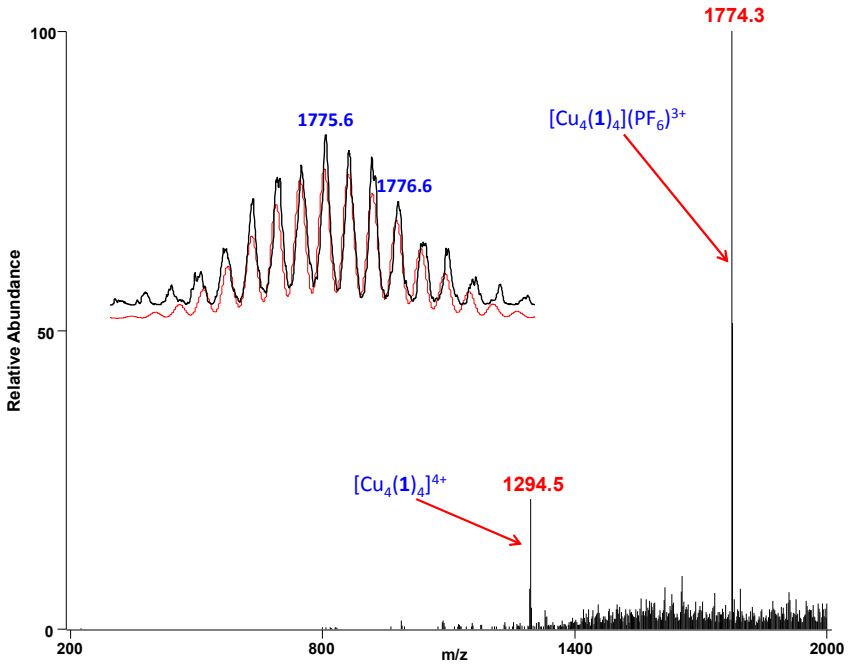

Figure S32: ESI-MS spectrum of square **S** = $[Cu_4(\mathbf{1})_4](PF_6)_4$ (in DCM) along with experimental (black) and calculated isotopic distributions (red) for the species $[Cu_4(\mathbf{1})_4](PF_6)^{3+}$.

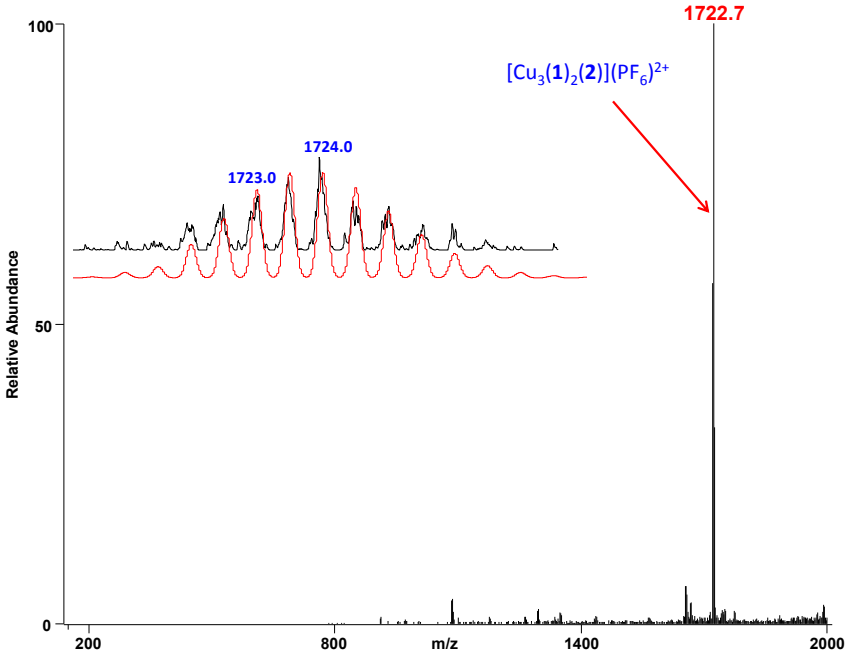

Figure S33: ESI-MS spectrum of triangle **T** = $[Cu_3(\mathbf{1})_2(\mathbf{2})](PF_6)_3$ (in DCM) along with experimental (black) and calculated isotopic distributions (red) for the species $[Cu_3(\mathbf{1})_2(\mathbf{2})](PF_6)^{2+}$.

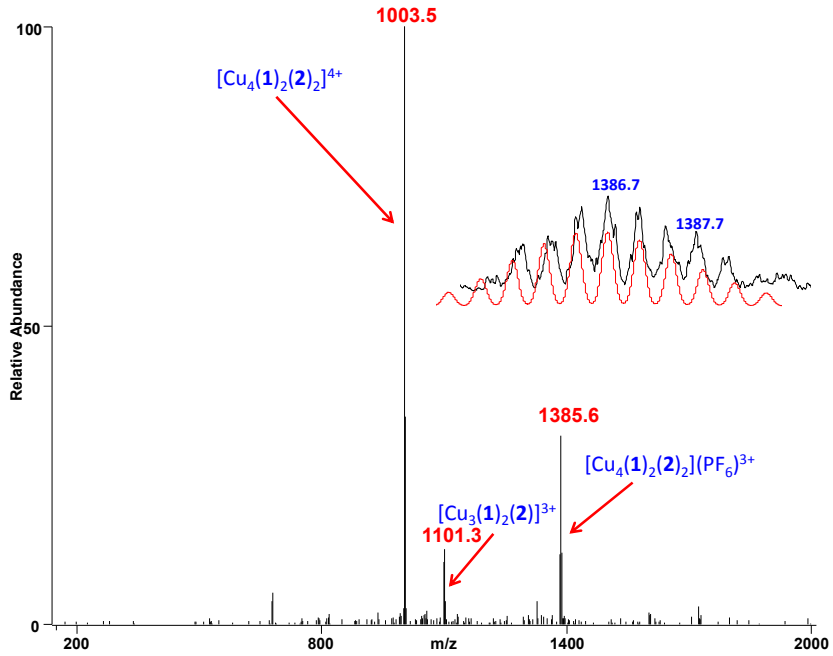

Figure S34: ESI-MS spectrum of rectangle **R** = $[Cu_4(\mathbf{1})_2(\mathbf{2})_2](PF_6)_4$ (in DCM) along with experimental (black) and calculated isotopic distributions (red) for the species $[Cu_4(\mathbf{1})_2(\mathbf{2})_2](PF_6)^{2+}$.

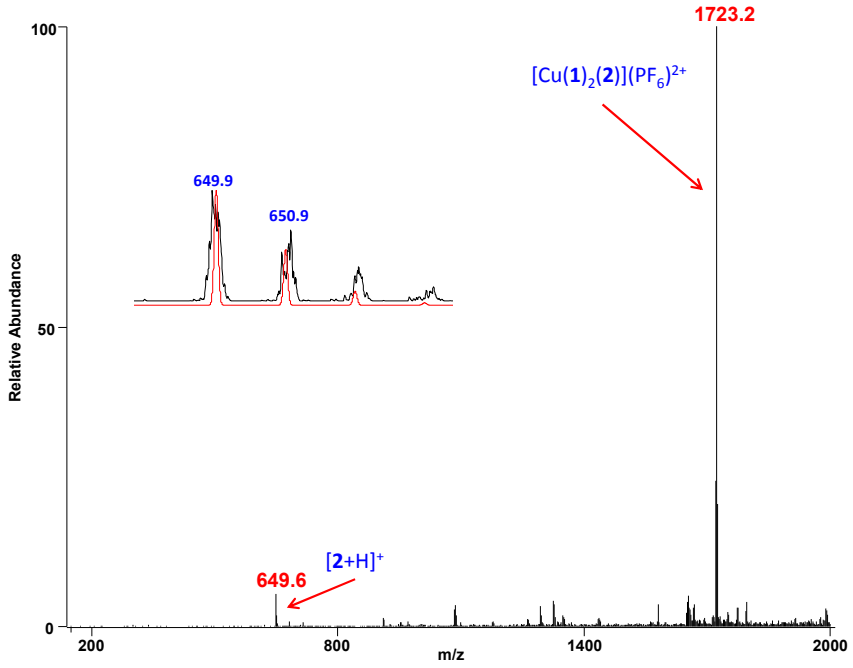

Figure S35: ESI-MS spectrum of state II (Scheme 1), as described in the manuscript, i.e. triangle **T** = $[Cu_3(\mathbf{1})_2(\mathbf{2})](PF_6)_3$ and free ligand **2** (in DCM) along with experimental (black) and calculated isotopic distributions (red) for the species $[\mathbf{2}+H]^+$.

Energy Minimised Structures

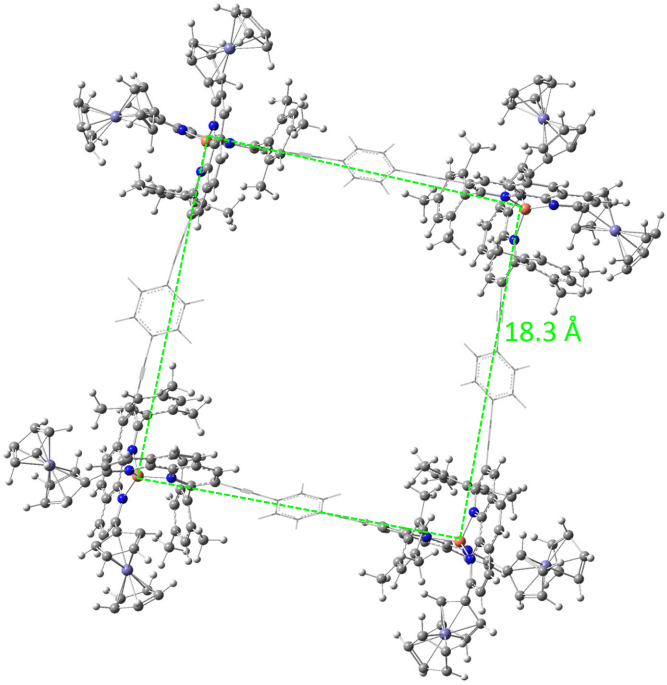

Figure S36: Energy minimised structure of the supramolecular square **S**. Counter anions and alkoxy chains are not included.

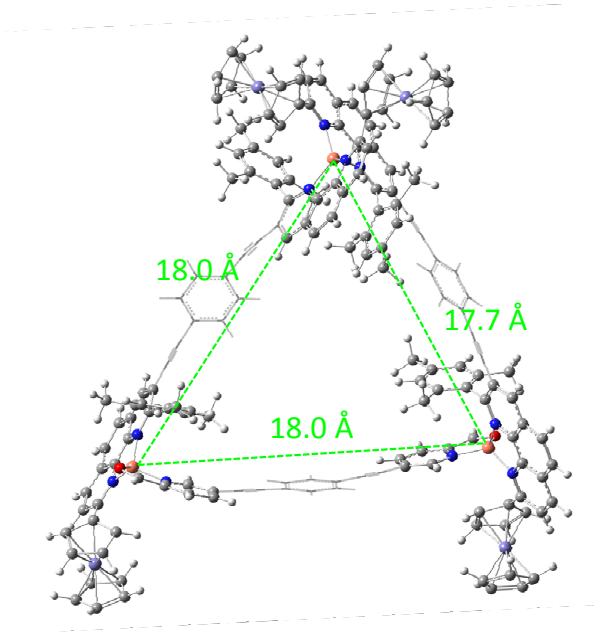

Figure S37: Energy minimised structure of the supramolecular isosceles triangle **T**. Counter anions and alkoxy chains are not included.

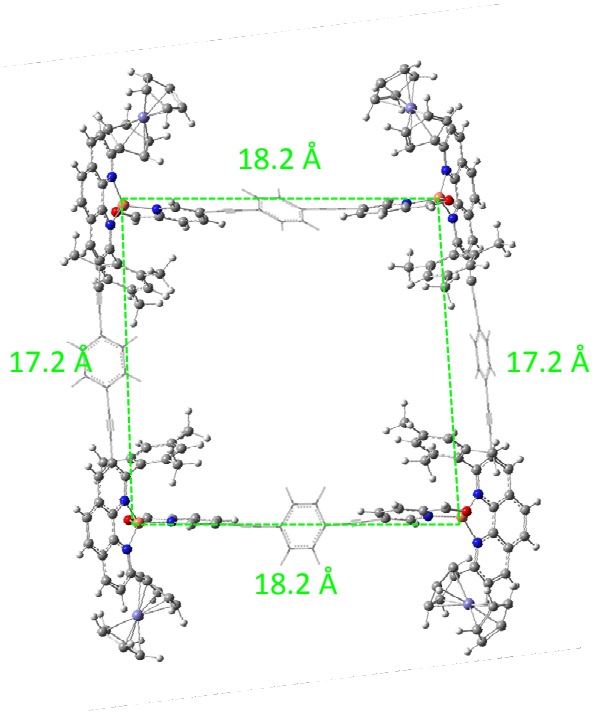

Figure S38: Energy minimised structure of the supramolecular rectangle **R**. Counter anions and alkoxy chains are not included.

References

1 M. Schmittel, M. L: Saha and J. Fan, *Org. Lett.*, 2011, **13**, 3916.

2 M. L. Saha, N. Mittal, J. W. Bats and M. Schmittel, *Chem. Commun.*, 2014, **50**, 12189.

3 Y. Zhou, Y. Yuan, L. You and E. V. Anslyn, *Chem. Eur. J.*, 2015, **21**, 8207.